Plant Cell Reports (2023) 42:1987–2010
https://doi.org/10.1007/s00299-023-03078-7

ORIGINAL ARTICLE

Nitrate-responsive transcriptome analysis of rice *RGA1* mutant reveals the role of G-protein alpha subunit in negative regulation of nitrogen-sensitivity and use efficiency

Jangam Annie Prasanna[1] · Vikas Kumar Mandal[1,2] · Dinesh Kumar[3] · Navjyoti Chakraborty[1] · Nandula Raghuram[1]

Received: 30 July 2023 / Accepted: 19 September 2023 / Published online: 24 October 2023

Abstract

Key message **Nitrate-responsive transcriptomic, phenotypic and physiological analyses of rice *RGA1* mutant revealed many novel *RGA1*-regulated genes/processes/traits related to nitrogen use efficiency, and provided robust genetic evidence of *RGA1*-regulation of NUE.**

Abstract Nitrogen (N) use efficiency (NUE) is important for sustainable agriculture. G-protein signalling was implicated in N-response/NUE in rice, but needed firm genetic characterization of the role of alpha subunit (*RGA1*). The knock-out mutant of *RGA1* in *japonica* rice exhibited lesser nitrate-dose sensitivity than the wild type (WT), in yield and NUE. We, therefore, investigated its genomewide nitrate-response relative to WT. It revealed 3416 differentially expressed genes (DEGs), including 719 associated with development, grain yield and phenotypic traits for NUE. The upregulated DEGs were related to photosynthesis, chlorophyll, tetrapyrrole and porphyrin biosynthesis, while the downregulated DEGs belonged to cellular protein metabolism and transport, small GTPase signalling, cell redox homeostasis, etc. We validated 26 nitrate-responsive DEGs across functional categories by RT-qPCR. Physiological validation of nitrate-response in the mutant and the WT at 1.5 and 15 mM doses revealed higher chlorophyll and stomatal length but decreased stomatal density, conductance and transpiration. The consequent increase in photosynthesis and water use efficiency may have contributed to better yield and NUE in the mutant, whereas the WT was N-dose sensitive. The mutant was not as N-dose-responsive as the WT in shoot/root growth, productive tillers and heading date, but equally responsive as WT in total N and protein content. The *RGA1* mutant was less impacted by higher N-dose or salt stress in terms of yield, protein content, photosynthetic performance, relative water content, water use efficiency and catalase activity. PPI network analyses revealed known NUE-related proteins as *RGA1* interactors. Therefore, *RGA1* negatively regulates N-dose sensitivity and NUE in rice.

Keywords G-protein signalling · Nitrogen response · Nitrogen use efficiency · Nitrate · Transcriptome · *Oryza sativa* · PPI network

Abbreviations

NUE	Nitrogen use efficiency
N	Nitrogen or nitrate
WUE	Water use efficiency
PPI	Protein–protein interaction

Communicated by Li Tian.

Jangam Annie Prasanna and Vikas Kumar Mandal have contributed equally to this work.

✉ Navjyoti Chakraborty
nchakraborty@ipu.ac.in

✉ Nandula Raghuram
raghuram@ipu.ac.in

[1] Centre for Sustainable Nitrogen and Nutrient Management, School of Biotechnology, Guru Gobind Singh Indraprastha University, Sector 16C, Dwarka, New Delhi 110078, India

[2] Prof. H.S. Srivastava Foundation for Science and Society, 10B/7, Madan Mohan Malviya Marg, Lucknow, India

[3] Division of Agronomy, ICAR-Indian Agricultural Research Institute, Pusa Campus, New Delhi, India

Introduction

Nitrogen is quantitatively the most important nutrient needed for plant growth and crop productivity. Most of the N-inputs remain unutilized due to the low N-use efficiency (NUE) of crop plants (Raghuram and Sharma 2019). This leads to N-pollution affecting air, water and soil quality, health, biodiversity and climate change, apart from wastage of fertilizers worth billions of dollars globally (Abrol et al. 2017; Sutton et al. 2019). The India-led United Nations Environment Assembly resolutions 4/14 (and 5/2) on sustainable nitrogen management called for improving NUE in all relevant sectors including agriculture (Raghuram et al. 2021).

NUE may be partly improved by agronomic and crop management practices, but biological interventions are needed for crop improvement (Udvardi et al. 2021; Raghuram et al. 2022). Considerable understanding has accumulated on the physiology, biochemistry and molecular biology of N-response (Pathak et al. 2008; Krapp 2015; O'Brien et al. 2016; Vidal et al. 2020; Xu and Takahashi 2020; Hou et al. 2021). However, the mechanisms of its regulation and the biological determinants of NUE are yet to be fully identified, even as tentative gene targets are being explored for NUE improvement (Mandal et al. 2018; Raghuram and Sharma 2019; Móring et al. 2021; The et al. 2021; Zhang et al. 2021; Madan et al. 2022). Rice is an ideal crop for improving NUE, not only due to its lowest NUE and highest N-fertilizer consumption among cereals globally, but also due to its huge germplasm and genomic resources (Li et al. 2017). Moreover, the phenotype for NUE has recently been characterized using experimental differentiation between N-response and NUE (Sharma et al. 2018, 2021).

Functional genomics of N-response revealed the involvement of thousands of genes beyond those directly involved in N uptake, assimilation, translocation and remobilisation in various crops, including rice (Chen et al. 2020; Pathak et al. 2020; Meng et al. 2021; Gao et al. 2022; Mandal et al. 2022 and references therein). Linking the phenotype and QTL information with transcriptomic data on N-response and yield, a few NUE gene targets in rice have been shortlisted (Kumari et al. 2021). They include signalling and regulatory targets, which figure prominently in many studies (Yang et al. 2017; Fredes et al. 2019; Nazish et al. 2021; Wang et al. 2021; Javed et al. 2022; Madan et al. 2022; Shanks et al. 2022; Xing et al. 2022).

Heterotrimeric G-protein signalling has been long implicated in nitrate-responsive gene expression in crop plants such as maize (Raghuram and Sopory 1999), rice (Ali et al. 2007; Liang et al. 2018; Zhu et al. 2020) and even in NUE in rice (Sun et al. 2014). Transcriptomic analyses of *Arabidopsis* single and double knock-out mutants of G-protein coupled receptor (*GCR1*) and Gα subunit (*GPA1*) also revealed significant effects on N-responsive genes/processes (Chakraborty et al. 2015b, 2019). Further, many of the G-protein regulated biological processes overlap with nitrate regulated processes such as meristematic growth, root system architecture, leaf development and stress (Yadav et al. 2013; Urano et al. 2014; Choudhury et al. 2020; Maruta et al. 2021, Yantong et al. 2022; Tiwari and Bisht 2022; Majumdar et al. 2023). Others include nodule formation, seed germination, seedling development, grain size, defense response, hormone signalling, redox homeostasis, light sensing and response and yield (Choudhury and Pandey 2016; Stateczny et al. 2016; Tian et al. 2018; Pandey and Vijayakumar 2018; Bhatnagar and Pandey 2020; Cui et al. 2020; Pathak et al. 2021; Zait et al. 2021; Zhang et al. 2021).

However, conclusive genetic evidence on the role of Gα (*RGA1*) subunit in N-response/NUE and its detailed molecular characterization were lacking. Therefore, the present study examined genomewide nitrate response in the rice *rga1* knock-out mutant relative to its corresponding wild type to conclusively address the role of *RGA1* in N-response/NUE and validated it at phenotypic, physiological and biochemical levels.

Materials and methods

Plant material and growth conditions

Seeds of wild type (WT) and *rga1* knock-out mutant of rice (*O. sativa* ssp. *japonica* cv. Nipponbare) were procured from the Faculty of Agriculture, Kyushu University, Japan and grown as described earlier (Mandal et al. 2022). This natural *d1* mutant containing a loss of function allele for *RGA1* was earlier characterized by Ashikari et al. (1999). Briefly, the surface-sterilized seeds were germinated on moist cotton in plastic trays in a plant growth chamber (PGC) at 25 ± 2 °C, with 75% relative humidity and light intensity of 2800 ± 100 Lux and a photoperiod of 12:12 h. Seedlings were then transplanted to 6-inch pots containing 1:1 mixture of soilrite and vermiculite and watered for the initial 10 days. Thereafter, seedlings were supplemented with 30 ml of 1X modified Arnon–Hoagland (AH) nutrient solution (pH 5.6–5.8) (Hoagland and Arnon 1950) every alternate day for the next 20 days. The media contained 5 mM each of KNO_3 and $Ca(NO_3)_2$, 1 mM KH_2PO_4, 2 mM $MgSO_4$, 46 µM H_3BO_3, 9 µM $MnCl_2{\cdot}4H_2O$, 0.765 µM $ZnSO_4{\cdot}7H_2O$, 0.32 µM $CuSO_4{\cdot}5H_2O$, 0.111 µM $H_2MoO_4{\cdot}H_2O$, 0.1 mM $FeSO_4{\cdot}7H_2O$ and 0.1 mM Na_2EDTA. These WT and mutant plants were either treated as following after 1 month post-transplantation for nitrate-responsive transcriptomic

analyses or grown till the end of the life cycle for physiological, yield and NUE measurements.

To test the effect of added nitrate, we needed a control of no added nitrate. As the plant cannot be grown for 30 days without nitrate and endogenous nitrate cannot be removed, we stopped nitrate supply for 2 days to bring down the nitrate response to the basal or control level as was done earlier by others (Krouk et al. 2010). To create N-depleted conditions, the pots were flushed with excess of ultrapure water followed by N-free 1X Arnon Hoagland (AH) media twice a day for 2 days. Leaf tissues were harvested on the 32nd day after transplantation and treated with either 120 mM KNO_3 (treatment) or 120 mM KCl (control) in Petri plates for 90 min. The concentration and duration of *in vitro* treatment were standardized earlier using nitrate dose–response studies on nitrate reductase and nitrite reductase activities & transcripts in rice (Pathak et al. 2020; Mandal et al. 2022). The use of excised leaves for nitrate treatment ensured that the measured short-term N-response is attributable to locally supplied nitrate and not to its downstream metabolite (Wang et al. 2004), nor is influenced by soil microbial conversions or root–shoot translocation issues (Pathak et al. 2020; Mandal et al. 2022). The leaf tissues from independent biological triplicates of both control and treatment WT and *rga1* mutants were then frozen in liquid nitrogen and stored at −80 °C till further use.

Phenotypic and physiological measurements

N-responsive physiological parameters were assessed in WT and mutant plants using three independent experimental replicates in the plant growth chamber (PGC). Briefly, germinated seedlings (WT and *rga1* mutants) were initially grown hydroponically in ultrapure water for 10 days in a growth chamber at 25 ± 2 °C, with 75% relative humidity and 98 µmol m^{-2} s^{-1} mean light intensity. For 10 more days they were treated with 1X AH nutrient solution with either 15 mM N or 1.5 mM N. These doses were achieved using a combination of $Ca(NO_3)_2$ and KNO_3 in the AH nutrient solution for 15 mM nitrate level, whereas for 1.5 mM nitrate level, only $Ca(NO_3)_2$ was used. The root and shoot lengths of the seedlings were measured before transplanting them into separate 2L cylindrical pots containing 1:1 mixture of soilrite and vermiculite and supplemented with either 1.5 and 15 mM N. The media were replenished every 48 h till the emergence of panicle and every 72 h thereafter. The data on shoot lengths, number of tillers, days to panicle emergence, numbers of panicles and weight of filled grains per plant were recorded.

Photosynthesis, stomatal conductance and transpiration rates were measured at the active tillering stage using LI-6400XT Portable Photosynthesis System (LI-COR® Biosciences, USA). Net photosynthetic CO_2 assimilation rate (µmol CO_2 m^{-2} s^{-1}) was measured with maximum light intensity falling at the plant level inside PGC (98 µmol m^{-2} s^{-1}). The reference CO_2 concentration was maintained at 410 ± 20 µmol mol^{-1} and all measurements were recorded during maximal photosynthetic activity between 12:00 noon till 4:00 p.m. IST (Indian Standard Time). Leaf chlorophyll content was determined as described by Lichtenthaler (1987).

Total N and protein content were determined as per Prasad et al. (2006). Briefly, the shoot samples were harvested after the full life cycle, dried at 90 °C and cut into small pieces. 0.5 g of the tissue was digested using conc. H_2SO_4 along with catalysts anhydrous sodium sulphate and dry copper sulphate pentahydrate. The total *N* and protein content were determined using the following formulae:

$$\text{Amount of } N\,(g) \text{ in sample } (S) = (V_s - V_a) \times \text{Na} \times 0.014,$$

where V_s = Volume of acid used for sample; V_a = Volume of acid used for blank; Na = Normality of acid.

$$\%N \text{ in sample} = \frac{S \times 100}{\text{Weight of sample (g)}}$$

$$\text{Crude Protein}\% = \%N \text{ in sample} \times 6.25$$

Total P and K content were determined as described by Prasad et al. (2006). Relative water content (RWC) and catalase activity were also calculated at the harvest stage. For measuring RWC, leaf samples from control and treated plants were harvested and their fresh weights (FW) were recorded (Chakraborty et al. 2015c). The leaves were then floated in distilled water for overnight in a covered Petri plate. Leaves were then removed from water and the surface was dried using a filter paper and their turgid weights (TW) were then recorded. Subsequently, the leaf samples were dried on filter paper in a hot air oven at 70 °C till a constant weight was reached. Dry weight (DW) of the leaf samples was recorded and RWC was calculated using the following formula:

$$\text{RWC}\,(100\%) = \left[\frac{(\text{FW} - \text{DW})}{(\text{TW} - \text{DW})} \times 100\right].$$

For measuring catalase activity, 100 mg rice leaf tissue was homogenized to fine powder in liquid nitrogen using pre-chilled mortar and pestle. Tissue homogenate was transferred to a sterile microcentrifuge tube (MCT) containing 400 µl of 0.1% TCA at 4 ºC. The solution was mixed by vortexing and then centrifuged at 12,000×*g* for 15 min at 4 °C. 200 µl of the supernatant was taken in a separate MCT and to it 100 µl of 10 mM potassium phosphate (K_3PO_4) buffer (at pH 7.0) and 200 µl 1 M potassium iodide (KI) were added and vortexed. Absorbance of samples was recorded

at 390 nm (Loreto and Velikova 2001). Final calculations were done by comparison with a standard curve of H_2O_2 (0.00–0.10 mM) prepared in 10 mM K_3PO_4 (at pH 7.0) and 1 M KI.

For salt stress responses, surface-sterilized and presoaked seeds of WT and *rga1* mutants were germinated in ultrapure water in a growth chamber under the growth conditions described above. Ten days after germination, seedlings were grown in 1X AH nutrient solution with nitrate concentrations 10 and 100% of the recommended N (1.5 mM and 15 mM N) for the full life cycle. Seedlings were grown in separate 2 L cylindrical pots with 1:1 mixture of soilrite and vermiculite to complete their life cycle in a PGC at 25 °C, with 75% relative humidity, 200 µmol m^{-2} s^{-1} light intensity and 12/12 h photoperiod. The nutrient solutions were replenished every 48 h till panicle emergence and every 72 h thereafter. After panicle emergence, plants were subjected to salt stress with 120 mM NaCl in AH nutrient solutions (Qu et al. 2012; Li et al. 2017; Chen et al. 2022) for 1 month during the grains filling stage and then leaf tissues were harvested. The data on total sodium, nitrogen, protein (Prasad et al. 2006) and relative water content, photosynthetic parameters and grain yield were recorded for the control and treated plants.

Scanning electron microscopy

Stomatal density and size were measured by scanning electron microscopy (SEM) at the UNESCO Regional Centre for Biotechnology, Faridabad, India. For this, 50-day-old leaf samples were used from three each of the 15 and 1.5 mM nitrate-treated WT and mutant plants. Each plant was sampled twice. Leaves were fixed for 2 h in 2% Karnovsky solution (2% glutaraldehyde and 2% paraformaldehyde in 0.1 M phosphate buffer). They were washed thrice for 15 min using 0.1 M phosphate buffer followed by dehydration for 15 min each, using gradually increasing concentration of AR-grade acetone (30–99.5%). Final dehydration was carried out using 100% acetone twice for 30 min each and critical point drying (CPD) was carried out using CO_2 followed by sputter coating with gold (18 mA for 15 s). The SEM was carried out using Apreo VS FESEM, FEI and the final images were obtained using xT Microscope Server 13.5.0 software.

RNA extraction, microarray analyses and data processing

Total RNA was isolated from frozen independent biological triplicates of control (120 mM KCl) and N-treated (120 mM KNO_3) leaf tissues using TRIzol reagent (Invitrogen, USA) as per manufacturer's instructions and processed for microarray analysis at Genotypic Technologies, Bengaluru, India. The quantity and quality of the extracted RNA were analyzed using Nanodrop spectrophotometer and Bioanalyzer (Agilent technologies, Santa Clara, USA). Samples having RIN value above 6 were used for microarray analysis with Agilent 8 × 60k rice arrays customized to include probes for nuclear and organellar genes. The mRNAs were transcribed into Cy3 labelled cRNAs, purified, checked for specific activity and then hybridized as per manufacturer's instructions. Agilent Feature Extraction software (version 9.1) was used and data were subjected to global normalization using the 75th percentile shift method. The raw data were deposited to NCBI–GEO database under the accession id GSE62164. Transcripts showing geometric mean fold change value ± 1.0 (log2FC) with statistically significant cut off (Benjamini Hochberg FDR ≤ 0.05) were considered as differentially expressed genes (DEGs) in the nitrate-treated samples with respect to the control (KCl) samples.

Functional classification of DEGs and data analysis

The nitrate-responsive DEGs in the mutant were subjected to GO enrichment analyses using EXPath 2.0 and REVIGO with default parameters; and AgriGO with hypergeometric test method and Hochberg (FDR) as the multi-test adjustment method. The statistically stringent FDR (<0.05) value was used to detect the significantly enriched GO terms. The MapMan tool was used to identify the pathways associated with DEGs. The DEGs were also mapped to various cellular pathways using KEGG (Kanehisa and Goto, 2000), RAP-DB database (https://rapdb.dna.affrc.go.jp/), Rice Genome Annotation Project database (http://rice.uga.edu/), PlantMetGenMap (http://bioinfo.bti.cornell.edu/cgi-bin/MetGenMAP/home.cgi) and Gramene (http://pathway.gramene.org/). DEGs were assigned to various morphological and agronomic traits like leaf, culm, panicle, yield and productivity using Oryzabase database (https://shigen.nig.ac.jp/rice/oryzabase/) and published literature. Heat maps were generated using Heatmapper online tool (http://heatmapper.ca/). Protein subcellular localization was predicted using CropPAL2.0 database (Hooper et al. 2016) using default parameters for rice. Differentially regulated transcription factors (TFs) were identified using comparison with STIFDB2 (Priya and Jain, 2013) and plantTFDB 4.0 (Jin et al. 2016).

Construction of protein–protein interaction networks and detection of molecular complexes

The interacting proteins for the DEGs were retrieved from STRING-DB (https://string-db.org/), MCDRP (http://www.genomeindia.org/biocuration/), BioGRID (https://thebiogrid.org/) and PRIN (http://bis.zju.edu.cn/prin/) databases. Only experimentally validated interactions were considered and DEGs were mapped to the protein–protein interaction

(PPI) networks constructed using Cytoscape version 3.8.2. To detect the molecular complexes, we used molecular complex detection (MCODE) plugin in Cytoscape network and chose the clusters with MCODE score > 3 with node number > 10 for further analysis.

Metadata analysis/comparison with wild type data

The current list of DEGs in the mutant was compared by Venn Selection with nitrate-responsive transcriptome datasets generated in the WT (Sawaki et al. 2013; Coneva et al. 2014; Misyura et al. 2014; Yang et al. 2015; Shin et al. 2018; Pathak et al. 2020; Mandal et al. 2022). Similar metadata analysis was also performed using the previously published *RGA1* transcriptomes (Ferrero-Serrano et al. 2018; Pathak et al. 2021) with the current data.

Validation of selected *RGA1*-regulated nitrate-responsive genes by RT-qPCR

Leaf tissues for RT-qPCR experiments were either obtained after in vitro nitrate treatment as described above for microarray experiments, or after in vivo N-treatments in intact plants as described for physiological experiments above. The nitrate doses were either 15 mM or 1.5 mM. Leaves harvested at the active tillering stage were used for RNA isolation and 5 µg each of total RNA was reverse transcribed into cDNA using PrimeScript 1st strand cDNA synthesis kit (TAKARA, Japan). To validate the differential expression of selected genes, RT-qPCR reaction was carried out in 10 µl volume using 1 µl of undiluted cDNA, 0.2 µl of forward and reverse primers (exon-junction spanning) (10 µM) and 5 µl of KAPA SYBR FAST Master Mix (2X) Universal (Kapa Biosystems, USA) in AriaMx Real-Time PCR System (Agilent Technologies, USA). The relative changes in gene expression were quantified by $2^{-\Delta\Delta}$CT method using actin genes (LOC_Os01g64630 and LOC_Os03g50885) as internal controls. Melting curve analyses of the amplicons were used to determine the specificity of RT-qPCR reactions. Experiments were performed using independent biological and technical triplicates.

Statistical analysis

The data were analyzed either by one-way or two-way ANOVA using GraphPad Prism ver. 6 (GraphPad Software, San Diego, CA). All the results were expressed as mean ± SEM from at least three replicates. Same letters denote statistically non-significant pairs.

Results

RGA1 mutation affects N-response and NUE

The main impetus for a detailed study of genomewide nitrate response in *rga1* mutant relative to the WT came from our meta-analysis of nitrate-responsive transcriptomes and *RGA1*-regulated transcriptomes, as they were never analyzed together. Venn selections were done using all the reported 5128 *RGA1*-regulated DEGs (Ferrero-Serrano et al. 2018; Pathak et al. 2021) with 23,926 N-responsive DEGs compiled from 7 published nitrate-transcriptomes in WT rice (Sawaki et al. 2013; Coneva et al. 2014; Misyura et al. 2014; Yang et al. 2015; Shin et al. 2018; Pathak et al. 2020; Mandal et al. 2022). We identified 3839 DEGs as both N-responsive as well as *RGA1*-regulated (Fig. 1a). Moreover, our pot experiments revealed that the mutant exhibited lesser nitrate-dose sensitivity than wild type (WT), in yield and NUE. (Fig. 1b, c). This also translates into enhancement of NUE in the mutant (Fig. 1c). *RGA1* mutation seems to have rendered the rice plants unresponsive or insensitive to higher N-dose, indicating the role of *RGA1* in negative regulation of N-sensitivity and NUE in the WT. These findings prompted a direct comparison of genomewide nitrate-response in the mutant and the WT.

RGA1 mutation alters genomewide nitrate-responsive gene expression

Nitrate is an important source of N for all plants including rice, even though it was adapted to tolerate ammonium (Bloom 2015; Kronzucker et al. 1999). Farm soils contain a dynamic mixture of different N-forms due to microbial conversions and fertilizers containing different N-forms, so we specifically designed our experiments with nitrate as the only form of N-supply and provided it directly to the target tissue (leaf) as a transient treatment to study N-responsive transcriptome. Excised leaves of 32 days old WT and *rga1* mutant deficient in G-protein α subunit (Ashikari et al. 1999; Pathak et al. 2021) were treated in vitro with KNO_3 or KCl prior to RNA isolation and simultaneous microarray analysis. The nitrate-responsive genes identified in the WT (KCl vs. KNO_3) were reported and analyzed separately in Mandal et al. (2022) and used as the baseline data for the current analysis of nitrate-responsive genes identified in the *RGA1* mutant (KCl vs. KNO_3). Scatterplot analysis revealed high correlations among our replicates,

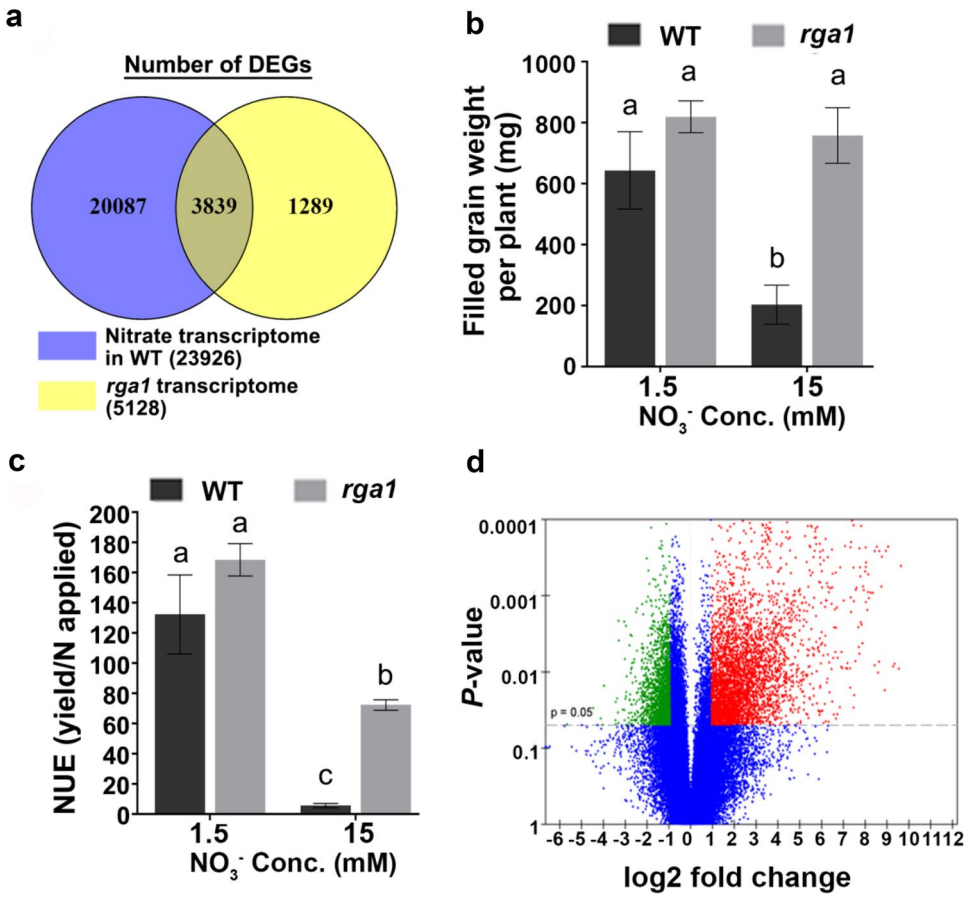

Fig. 1 N-responsive genes and yield and NUE measurements of rice WT and *rga1* mutant (*d1*) in response to two different doses of nitrate. **a** Venn diagram showing the unique and common DEGs identified in published seven nitrate-responsive transcriptomes in wild type (WT) (Sawaki et al. 2013; Coneva et al. 2014; Misyura et al. 2014; Yang et al. 2015; Shin et al. 2018; Pathak et al. 2020; Mandal et al 2022) and *rga1*-responsive transcriptomes (Ferrero-Serrano et al. 2018; Pathak et al. 2021). **b** Bar graph representing the total weight of filled grains per plant in WT and *rga1* mutant plants grown in pots with two different concentrations of nitrate. **c** Bar graph representing the total NUE per plant in WT and *rga1* mutant plants grown in pots with two different concentrations of nitrate. **b**, **c** Each bar graph represents mean ± SE of the data from twelve biological replicates. The statistical significance is calculated using two-way ANOVA in GraphPad Prism 6.0 and same letters denote non-significant pairs. **d** Volcano plot showing the distribution of all genes across their log2 fold change in the current *rga1* nitrate transcriptome. The red and green coloured spots represents up- and downregulated DEGs enriched based on geometric mean fold change value ± 1.0 (log2FC) with statistically significant cut off (Benjamini–Hochberg FDR ≤ 0.05)

indicating the uniformity of results across replicates (Supplementary Fig. 1). A total of 3416 genes showed differential expression (2245 upregulated and 1171 downregulated) in response to nitrate treatment in the mutant, as visualized in the volcano plot (Fig. 1d). The complete list of DEGs is provided in Supplementary Table 1. The table also reveals 4 upregulated and 11 downregulated miRNAs that show significant N-response in the transcriptome. Overall, our data clearly show that *RGA1* mutation has an extensive genome-wide impact on nitrate-responsive gene expression.

Meta-analysis reveals common and unique N-responsive genes in *RGA1* mutant

We compared our list of 3416 nitrate-responsive DEGs in the *rga1* mutant (relative to KCl) with those from two published *rga1* mutant transcriptomes that did not consider N and seven WT nitrate-transcriptomes that did not consider *rga1* (Fig. 2a). The latter included one data set from the corresponding WT *japonica* under identical treatment conditions (Mandal et al. 2022). Our Venn selections delineated and confirmed at least 835 of the 3839 genes shared between nitrate-responsive transcriptomes and *RGA1*-regulated transcriptomes (Fig. 2a). In other words, these 835 genes were actually confirmed as nitrate-responsive in the

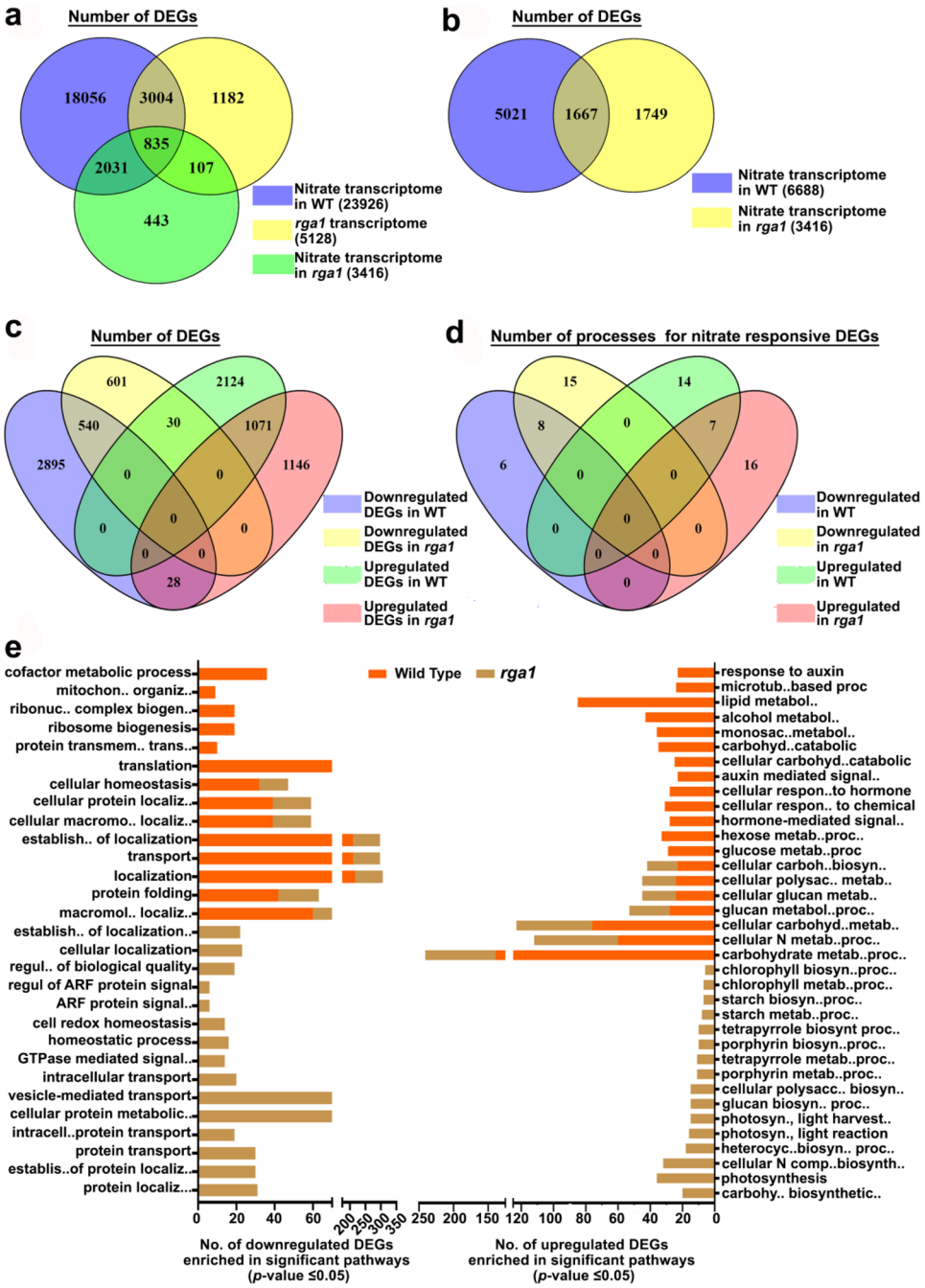

Fig. 2 N-responsive genes and their functional annotation. **a** Venn diagram showing the unique and common DEGs identified in published seven nitrate-responsive transcriptomes in WT and nitrate-responsive DEGs identified in *RGA1* mutant (*d1*). **b** Venn diagram showing the unique and common DEGs identified in the wild type (WT) (Mandal et al. 2022) and *rga1* mutant using microarray carried out under similar conditions. **c** Venn diagram showing the unique and common up- and downregulated genes identified in the *rga1* mutant and its corresponding WT using microarray carried out under similar conditions. **d** Venn diagram showing the unique and common biological processes identified in the *rga1* mutant and its corresponding WT using microarray carried out under similar conditions. **e** Bar chart showing the distribution of DEGs in statistically significant enriched pathways identified using AgriGOv2.0

mutant for the first time. There were an additional 2031 DEGs in the mutant that were common with the seven nitrate transcriptome datasets in WT; and an additional 107 DEGs common with the two *rga1* mutant transcriptomes. More importantly, our microarray revealed 443 novel *RGA1*-regulated N-responsive DEGs not reported in any earlier transcriptome (Fig. 2a).

A separate Venn selection of the nitrate-responsive DEGs in the *rga1* mutant *vs.* WT was done, as the WT data were obtained under identical conditions (Mandal et al. 2022). It revealed 1667 common DEGs, which were comparable in the nature and extent of their regulation by nitrate, especially in the mild to moderate levels of regulation (Fig. 2b, c). There were a few common DEGs with high levels of regulation that differed between the WT and mutant, especially among the downregulated DEGs. Interestingly, *RGA1* mutation rendered 5021 or 75% of the 6688 nitrate-responsive genes in the WT as unresponsive, while also rendering 1749 unresponsive genes in the WT as nitrate responsive. Further segregation of these novel 1749 DEGs into up- and

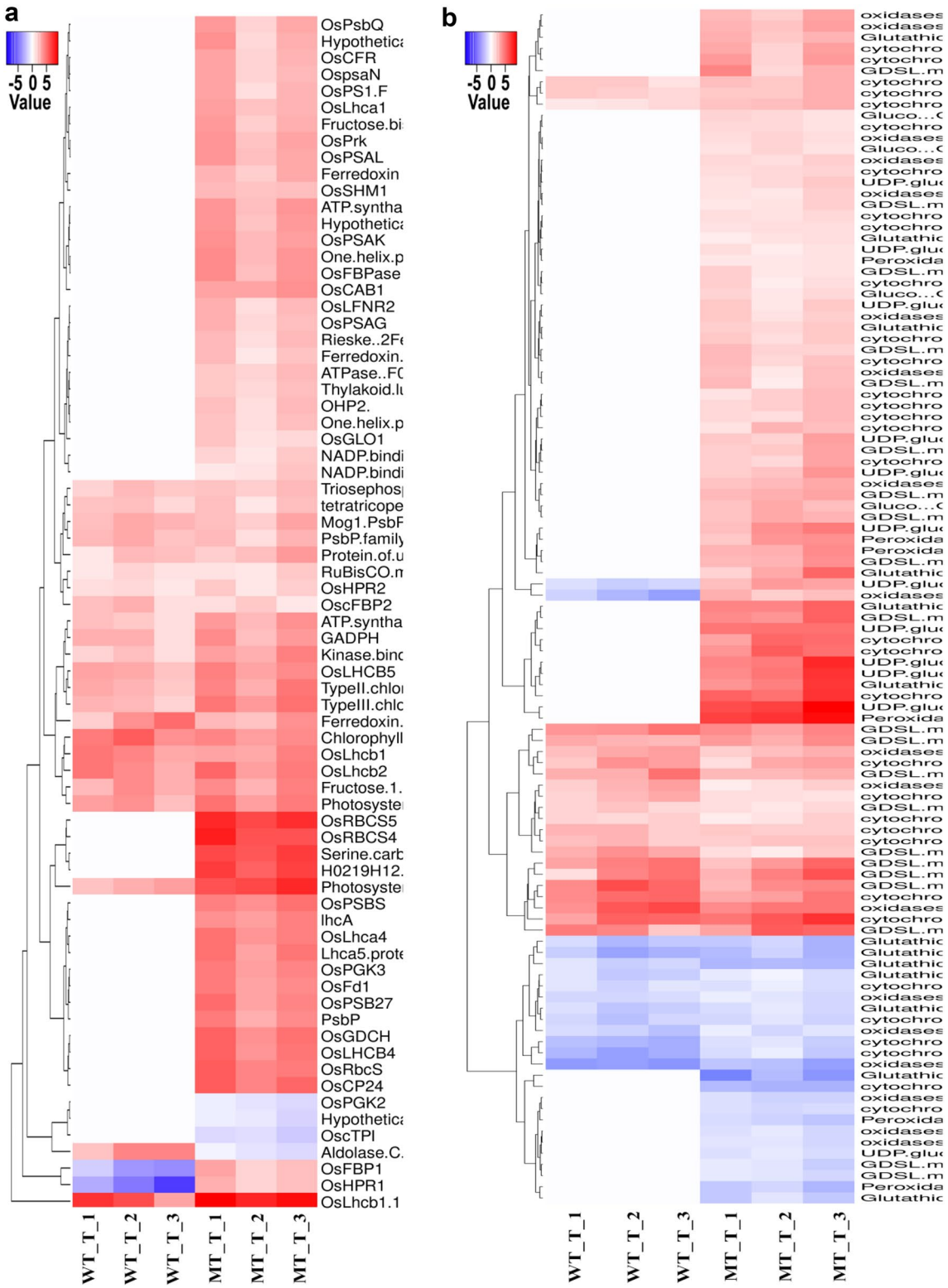
a
-5 0 5
Value
OsPsbQ
Hypothetica
OsCFR
OspsaN
OsPS1.F
OsLhca1
Fructose.bi
OsPrk
OsPSAL
Ferredoxin
OsSHM1
ATP.syntha
Hypothetica
OsPSAK
One.helix.p
OsFBPase
OsCAB1
OsLFNR2
OsPSAG
Rieske..2Fe
Ferredoxin.
ATPase..FC
Thylakoid.lu
OHP2.
One.helix.p
OsGLO1
NADP.bindi
NADP.bindi
Triosephos
tetratricope
Mog1.PsbP
PsbP.family
Protein.of.u
RuBisCO.n
OsHPR2
OscFBP2
ATP.syntha
GADPH
Kinase.binc
OsLHCB5
TypeII.chlo
TypeIII.chlc
Ferredoxin.
Chlorophyll
OsLhcb1
OsLhcb2
Fructose.1.
Photosyste
OsRBCS5
OsRBCS4
Serine.carb
H0219H12.
Photosyste
OsPSBS
lhcA
OsLhca4
Lhca5.prote
OsPGK3
OsFd1
OsPSB27
PsbP
OsGDCH
OsLHCB4
OsRbcS
OsCP24
OsPGK2
Hypothetica
OscTPI
Aldolase.C.
OsFBP1
OsHPR1
OsLhcb1.1
WT_T_1
WT_T_2
WT_T_3
MT_T_1
MT_T_2
MT_T_3
b
-5 0 5
Value
oxidases
oxidases
Glutathic
cytochro
cytochro
GDSL.m
cytochro
cytochro
cytochro
Gluco...C
cytochro
oxidases
Gluco...C
oxidases
cytochro
UDP.gluc
oxidases
GDSL.m
cytochro
cytochro
Glutathic
UDP.gluc
Peroxida
GDSL.m
cytochro
Gluco...C
UDP.gluc
oxidases
Glutathic
cytochro
GDSL.m
cytochro
oxidases
GDSL.m
cytochro
cytochro
cytochro
cytochro
UDP.gluc
GDSL.m
cytochro
UDP.gluc
oxidases
GDSL.m
Gluco...C
GDSL.m
UDP.gluc
Peroxida
Peroxida
GDSL.m
Glutathic
UDP.gluc
oxidases
Glutathic
GDSL.m
UDP.gluc
cytochro
cytochro
UDP.gluc
UDP.gluc
Glutathic
cytochro
UDP.gluc
Peroxida
GDSL.m
GDSL.m
oxidases
cytochro
GDSL.m
oxidases
cytochro
GDSL.m
cytochro
cytochro
cytochro
GDSL.m
GDSL.m
GDSL.m
GDSL.m
cytochro
oxidases
cytochro
GDSL.m
Glutathic
Glutathic
Glutathic
cytochro
oxidases
Glutathic
cytochro
oxidases
cytochro
cytochro
oxidases
Glutathic
cytochro
oxidases
cytochro
Peroxida
oxidases
oxidases
UDP.gluc
GDSL.m
GDSL.m
Peroxida
Glutathic
WT_T_1
WT_T_2
WT_T_3
MT_T_1
MT_T_2
MT_T_3

◂**Fig. 3** Functional annotation of DEGs involved in photosynthesis and metabolism. **a** Heatmap showing the distribution of nitrate-responsive photosynthesis-related DEGs identified in the *rga1* mutant (*d1*) vs the corresponding WT. Gradient of red colour represents upregulated while gradient of blue represents the downregulated genes. The colour scale shows the log2FC values. **b** Heatmap showing the distribution of nitrate-responsive metabolism-related DEGs identified in the *rga1* mutant vs the corresponding WT. Gradient of red colour represents upregulated while gradient of blue represents the downregulated genes. The colour scale shows the log2FC values. The complete list of genes belonging to each functional category is provided in Supplementary Tables 6 & 7. We validated four DEGs belonging to photosynthesis (*OsCRY1a, OsLFNR2, Non-photo hypocotyl3* and *YL1*) as well as five belonging to abiotic stress response and/or metabolism (*OsDjC26, OsGS2, OsLACS1, Sugar/inositol transporter* and *OsADH1*) as shown in Fig. 5

downregulated sub-categories revealed 1146 and 601 DEGs, respectively, in the mutant (Supplementary Table 2). Overall, the upregulated genes are almost twice the number of downregulated genes, both among the common DEGs and those unique to the mutant (Fig. 2b, c).

After including gene Ids for 151 differentially expressed proteins from the previously published *rga1* mutant proteome dataset (Peng et al. 2019), the number of novel and exclusive *RGA1*-regulated N-responsive DEGs identified in the current study was 2453 (Supplementary Table 3).

Common and unique nitrate-responsive biological processes in WT and *rga1* mutant

Further Venn selections were performed with the process categories to ascertain the functional biological implications of the above 1749 uniquely up/downregulated genes identified in the mutant. This revealed 15 uniquely enriched biological processes for downregulated and 16 for upregulated nitrate-responsive DEGs in the *rga1* nitrate transcriptome (Fig. 2d, e). In other words, the seemingly huge differences in the number of up- and downregulated DEGs does not translate into comparable differences in the number of processes involved. This is true at least for the processes uniquely regulated by nitrate in the mutant (but not in the wild type). All the common and unique processes enriched for nitrate-responsive DEGs in WT and *rga1* datasets are shown in Fig. 2e.

AgriGO analyses revealed that the 2474 *RGA1*-regulated, nitrate-responsive DEGs identified exclusively in our study of the mutant (and not in the earlier studies) belonged to nine uniquely enriched processes as well as to ten previously known biological processes (Fig. 2e and Supplementary Table 4). Novel *RGA1*-regulated and N-responsive processes include regulation of biological quality (28 DEGs), porphyrin metabolism (8 DEGs), ARF protein signal transduction (7 DEGs), small GTPase mediated signal transduction (18 DEGs), tetrapyrrole metabolism (8 DEGs) and cofactor metabolism (21 DEGs). Further, additional/novel *RGA1*-regulated and N-responsive DEGs were identified belonging to ten known processes such as cellular nitrogen compound metabolism (41 additional), heterocycle biosynthesis (15 additional), homeostasis (23 additional), carbohydrate metabolism (83 additional), photosynthesis and light harvesting (6 additional).

To understand the overall biological roles of all the N-responsive DEGs found in the current study, they were subjected to GO analysis using the AgriGO ver. 2.0 (Tian et al. 2017) and REVIGO (Supek et al. 2011). Only the statistically over-represented terms for biological processes were used for further analysis (Fig. 2d, e; Supplementary Tables 3 and 4). Photosynthesis, carbohydrate biosynthesis, chlorophyll, tetrapyrrole and porphyrin biosynthesis and cellular nitrogen compound biosynthesis were among the 16 uniquely over-represented GO-BP terms for upregulated nitrate-responsive DEGs in the mutant. This was followed by seven common processes for upregulated DEGs in both mutant and WT nitrate-transcriptomes. These include carbohydrate metabolism, cellular nitrogen compound metabolism and glucan metabolism. For the downregulated nitrate-responsive DEGs unique to the mutant, 15 enriched GO terms were identified, including cellular protein metabolism, intracellular protein transport, small GTPase mediated signal transduction, cell redox homeostasis and regulation of biological quality. There were also eight processes common to downregulated DEGs in both WT and mutant datasets, including cellular protein localization, cellular homeostasis, protein folding and transport.

Further, statistically significant GO terms were also retrieved using gProfiler (Raudvere et al. 2019) and EXPath (Tseng et al. 2020). They revealed many similar but also a few additional process terms associated with uniquely N-responsive DEGs in the mutant viz., response to light stimulus, response to cytokinin, cell surface receptor signalling pathway, protein refolding, glutathione metabolism and cell wall biogenesis were the most significant among those processes (Supplementary Table 4). Photosynthesis, chlorophyll biosynthesis, carbohydrate metabolism and carboxylic acid metabolism were most over-represented in the upregulated DEGs, while protein transport (intracellular and vesicle-mediated), protein folding, cell redox homeostasis and regulation of ARF protein signal transduction were the most over-represented GO terms among the downregulated DEGs. All the DEGs were also mapped to various functional categories or 'bins' using MapMan (Thimm et al. 2004).

The results of MapMan analysis were highly correlated with those of AgriGO, EXPath and gProfiler. Metabolic processes, cellular response and photosynthesis were found

to be the bins to which a significant number of DEGs were mapped (Fig. 3). In addition to these, DEGs were also mapped to regulation, receptor like kinases and tetrapyrrole biosynthesis, among others (Supplementary Fig. 2). Further analysis of these bins revealed that most of the DEGs were mapped to important sub-bins like stress response (abiotic and biotic), development, cell wall, light reactions, secondary metabolism, RLKs (LRR, S-locus, WAK, PERK-like and DUF26; receptor like cytoplasmic kinases) (Supplementary Fig. 3). Pathway analysis using PlantMetGenMap (Joung et al. 2009) revealed 20 statistically significant differentially regulated pathways (Supplementary Table 5). These include cellulose biosynthesis, NAD salvage pathway II, β-D-glucuronide degradation, Calvin cycle, proline biosynthesis, etc. Most of the DEGs involved in these pathways showed upregulation.

Our search for processes (GO-BP terms) associated with the DEGs using AgriGO, EXPath and MapMan (Figs. 2e, 3, 4 and Supplementary Figs. 2 & 3) further elaborate the role of *RGA1* in the regulation of several N-responsive processes. AgriGO analysis revealed that all the genes related to carbohydrate metabolic process were upregulated by N treatment in WT (139) as well as in the mutant (102). However, there were 46 common genes in both the datasets and 71 and 41 unique genes in WT and mutant, respectively. Similarly, all the genes related to cellular nitrogen compound metabolic process were also upregulated in WT (60) and mutant (52) and there were 26 common and 26 unique DEGs in the mutant. Out of 51 DEGs involved in photosynthesis, which we earlier reported as N-responsive in WT plants, 25 were also common in the mutant dataset (total 72).

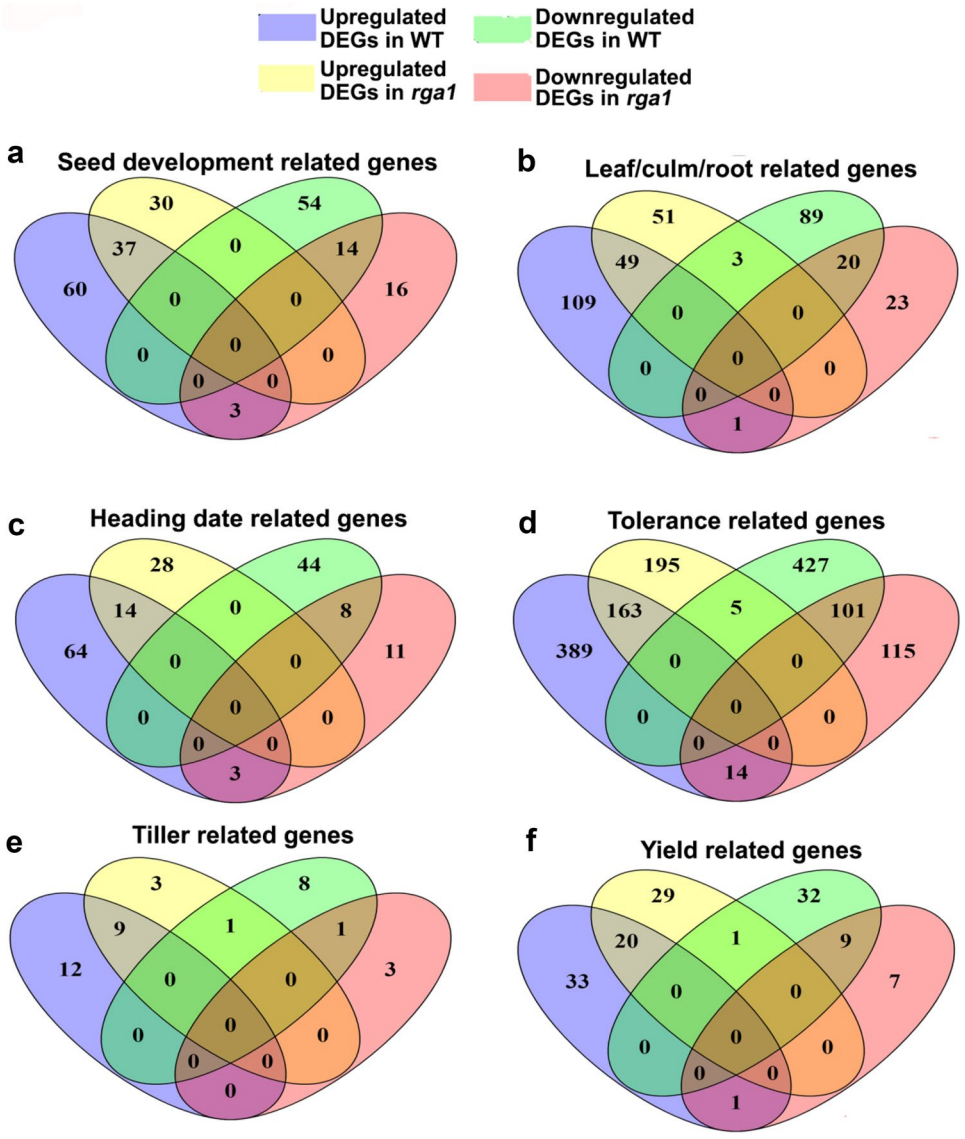

Fig. 4 Trait-related DEGs identified in the *rga1* mutant (*d1*) and the corresponding WT. **a**–**f** Venn selection to identify DEGs associated with different traits as indicated. DEGs were assigned to various morphological and agronomic traits like leaf, culm, panicle, yield and productivity using Oryzabase database (https://shigen.nig.ac.jp/rice/oryzabase/) and published literature. The complete gene list for each trait is provided in Supplementary Table 7 along with their fold change values. The selected DEGs (fourteen) belonging to N-responsive traits were validated by RT-qPCR as shown in Fig. 5 and mentioned in the following sections

RGA1 signalling mediates N regulation of agronomic traits

A total of 414 DEGs were mapped to the metabolic processes bin using MapMan (Supplementary Table 6; Supplementary Fig. 2). These included genes involved in carbohydrate, lipid, amino acid and nucleotide metabolism and cell wall biosynthesis (Supplementary Fig. 2 and Fig. 3b). Interestingly, Nitrate Transporter (*NRT2.6*) and Glutamate Synthase (*GOGAT*), the genes involved in N uptake and assimilation, which are known to be upregulated by nitrate, were found to be down-regulated in the mutant. Whereas, other primary N assimilation genes like Glutamine Synthetase (*GS*) and Glutamate Dehydrogenase (*GDH*) were upregulated in the mutant. This is by far the most compelling genetic evidence of the role of G-protein (*RGA1*) in nitrate response.

We also obtained 61 DEGs, which are involved in secondary metabolism like flavonoid and phenylpropanoid metabolism. Most of these DEGs were found to be upregulated, other than those involved in tetrapyrrole metabolism. Further, a total of 185 DEGs belonging to various large enzyme families like cytochrome P450, oxidases, nitrilases, UDP glucosyl and glucuronyl transferases, glutathione-S-transferases, alcohol dehydrogenases, etc. were identified in the analysis. 142 of these enzyme-related DEGs were upregulated, whereas 43 were downregulated in the *rga1* mutant. Their heatmap in Supplementary Fig. 13 and gene list in Supplementary Table 6 and Supplementary Table 7 show 90 unique DEGs related to these enzyme classes uniquely regulated by nitrate in the mutant. 79 DEGs related to biosynthesis and signalling of hormones like auxin, ABA, BR, ethylene, cytokinin, GA, jasmonic acid and salicylic acid were also identified (Supplementary Fig. 2).

Photosynthesis was found to be the most enriched category across analyses using all the *in-silico* tools. A total of 72 DEGs were mapped in the photosynthesis bin of MapMan (Fig. 3a). These include genes involved in light reactions, Calvin cycle as well as photorespiration. Heatmap for 47 unique DEGs (along with total) related to photosynthesis uniquely regulated by nitrate in the mutant is shown in Fig. 3. Out of total 72, 68 DEGs were upregulated, whereas only 4 were downregulated in the mutant (Fig. 3a).

Finally, on the basis of literature (Boonburapong and Buaboocha 2007; Gao and Xue 2012), MapMan and other database searches (RGAP, RAPdb, STIFDB2 and PlantTFDB), we prepared a list of non-redundant 857 DEGs across metabolism, signalling and transcriptional regulation categories. These DEGs were related to photosynthesis and/or enzymes and/or C and N metabolism and/or (TFs) and/or RLKs and/or G-proteins and/or MAP Kinases and/or hormones in the *rga1* nitrate transcriptome (Supplementary Fig. 7 and Supplementary Table 7). Interestingly, as many as 1536 N-responsive DEGs belonging to the same above categories were highly enriched with higher fold change in the WT but not in the mutant (Supplementary Table 7), indicating that nitrate response in the mutant and WT target the same processes through different genes.

The agronomically important traits associated with the *RGA1*-regulated and N-responsive DEGs such as root/shoot/tiller development, heading date/panicle emergence/flowering, seed development and yield are shown in Fig. 4 and Supplementary Fig. 13. The heatmaps (Supplementary Fig. 13) also indicate their involvement in metabolism and/or signalling and/or transcriptional regulation categories (Fig. 4 and Supplementary Fig. 7). Out of 147 DEGs for leaf/culm/ root development, 59 belonged to the abovementioned three functional categories (17 downregulated and 42 upregulated). Similarly, 21 (6 down- and 15 upregulated) and 46 DEGs (12 down- and 34 upregulated) belonging to these functional categories were identified for heading (64) and seed development (100), respectively. Additionally, these functional categories also make up 250 (87 down- and 163 upregulated), 29 (8 down- and 21 upregulated) and 5 (1 down- and 4 upregulated) DEGs for tolerance/resistance (581), yield/productivity (67) and tiller (17), respectively.

Further comparison revealed a smaller number of exclusive DEGs related to N-responsive agronomic traits in the mutant relative to the WT and their fold change was also lesser (Fig. 4 and Supplementary Table 7). There were in total 198 exclusive DEGs in WT related to leaf/culm/ root development compared to 74 exclusive in the mutant), 108 related to heading/inflorescence/panicle (39 exclusive in mutant), 114 related to seed development/yield (46 exclusive in mutant), 816 related to tolerance/resistance (296 exclusive in mutant) and 20 related to tiller development (6 exclusive in mutant). This means that 604 nitrate-responsive DEGs associated with agronomic traits in the WT were rendered unresponsive to nitrate due to the lack of functional *RGA1* in the mutant. This pattern is also reflected in the phenotypic responses in the mutant and WT as explained in later sections.

Subcellular distribution of DEGs and identification of associated transcription factors

To understand the effect of Gα knockout mutation on nitrate response at global cellular and subcellular levels, all DEGs were subjected to subcellular prediction using cropPAL2.0 program (Hooper et al. 2016). We found that most of the upregulated DEGs were distributed into cytosol (22%), plastid (21%), plasma membrane (12%) and extracellular (11%), among others (Supplementary Fig. 4); while most of the downregulated DEGs were distributed into cytosol (26%), plasma membrane (18.5%) and nucleus (15%) (Supplementary Fig. 4 and Supplementary Table 8).

This clearly suggests the involvement of *RGA1* in the regulation of pathways occurring in these multiple subcellular locations and organelles. Our search with the DEGs in STIFDB2, RGAP, PlantTFDB and MapMan databases revealed a total of 343 differentially regulated (TFs) (TFs) spread across 30 TF families (TFFs) with bZIP, NAC and bHLH TF being most over-represented. About 66% of the TFs were upregulated, while the rest of them (34%) were downregulated. Most of the TFs of bHLH, bZIP, HD-ZIP, GRAS, MYB-related and SBP TFFs were upregulated, while those of C2H2, ERF, Dof, WRKY and HSF TFFs were downregulated (Supplementary Table 7).

PPI network analysis revealed photosynthetic and metabolism as enriched clusters

We developed protein–protein interaction (PPI) networks and mapped the DEGs onto them to find *RGA1*-regulated interactions in nitrate response/NUE. The network was constructed using only the experimentally verified interaction data from STRING, MCDRP, BioGRID and PRIN databases and expression values of the DEGs were colour-coded to visualize the network using Cytoscape 3.8.2 (Shannon et al. 2003). The network consisted of 542 nodes and 1808 edges after removing the duplicated edges. As compared to the WT, the DEGs in the mutant formed a majority of the interacting proteins in the network, indicating the differences in functional interactions underlying nitrate response in the wild type and *RGA1* mutant (Supplementary Fig. 5 and S6 and Supplementary Table 9). MCODE analyses revealed four highly connected sub-clusters of molecular complexes having MCODE score > 3 with node number > 10 (Supplementary Fig. 6). A total of 32, 30, 12 and 11 nodes having 445, 402, 64 and 55 number of edges were found in the sub-cluster 1, 2, 3 and 4, respectively. Singular enrichment analysis (SEA) of the genes in these clusters using AgriGO revealed that genes of both clusters 1 and 2 are associated with "metabolism", "cellular biosynthesis" and "translation" (Supplementary Fig. 6). The genes of cluster 3 and 4 were found to be involved in "ubiquitin-dependent protein catabolic process" and "photosynthesis", respectively.

We also found a large network formed only of the validated interactors of *RGA1* (Supplementary Fig. 5 and S6). A majority of these interactors (46 out of 64) were found to be N-responsive when these interactors were screened against known N-responsive genes.

qPCR validation of DEGs across important biological processes

To validate the *RGA1* regulation of N-responsive DEGs selected from different functional categories identified in the microarray data (GSE62164), relative transcript abundance values of 12 upregulated DEGs and 6 downregulated DEGs were determined by qRT-PCR (Fig. 5a). The primer sequences for the DEGs validated in the experiment are provided in Supplementary Table 10. They were selected based on their involvement in important pathways such as regulation of cell division and cell cycle and/or DNA synthesis and repair and/or development (*OsSTA28*, *OsCYP37*, *CYP26-2*, *Zinc finger*, *FYVE-type domain containing protein, OsNYC3, Regulator of chromosome condensation, OsRPA1, Replication protein A1, OsRH16* and *OsRH10*). The expression patterns matched with the microarray data and the $\log_2$ fold changes for the eight DEGs (four upregulated and four downregulated) were significantly different in the mutant as compared to the WT (Fig. 5a). We also validated four DEGs belonging to light signalling and/or photosynthesis (*OsCRY1a, OsLFNR2, Non-photo hypocotyl3* and *YL1*) as well as five belonging to abiotic stress response and/or metabolism (*OsDjC26, OsGS2, OsLACS1, Sugar/inositol transporter* and *OsADH1*). Under these categories, the fold change for four upregulated and one downregulated DEGs were significantly different in the mutant as compared to the WT. Figure 5a shows the comparison of the nitrate-responsive gene expression after in vitro treatment of wild type vs. *rga1* mutant leaves. The figure also shows the upregulation of seven (*OsLFNR2, OsDjC26*, *OsGS2*, *OsSTA2*8 *OsCYP37*, *OsCYP26-2*, *Zn-finger FYVE*) and downregulation of two (*RCC*, *OsRPA1*) exclusive N-responsive DEGs in the mutant, whereas the expression for these DEGs was very close to the baseline '0' in the WT.

Further validation was done in whole plants, using the leaf tissues of WT and mutant plants at active tillering stage grown with either 1.5- and 15 mM nitrate. The differential expression of eight DEGs (Fig. 5b) was validated as upregulated viz. *OsSTA28*, *OsCYP26-2*, *OsDjC26*, *OsCAT-A*, *ALPHA-AMYLASE 3D*, *OsLhca3*, *OsFBP1* and *OsCDPK23*. Downregulated DEGs were also validated namely, *RNA Helicase*, *CLASS I CLP ATPASE B-M*, *OsGPDH1-1* and *Similar to Coatomer gamma subunit*. These DEGs belonged to cell cycle and/or DNA synthesis (*Os RH16*, *OsSTA28*, *OsCYP26-2*) and abiotic stress responses (*OsDjC26*, *OsCAT-A & CLASS I CLP ATPASE B-M*). Other DEGs belonging to photosynthesis/yield (*OsGPDH1-1*, *ALPHA-AMYLASE 3D, OsLhca3* and *OsFBP1*) and signalling or protein transport (*OsCDPK23, Similar to Coatomer gamma subunit*) were also validated. The expression patterns matched with the microarray data and fold changes of all these DEGs were significantly different in the mutant as compared to the WT (Fig. 5). These results clearly reveal that the *RGA1* and N regulation of the DEGs as observed in excised leaves was also valid in intact plants grown with normal dose of nitrate prescribed in AH solution. They also provide conclusive evidence for

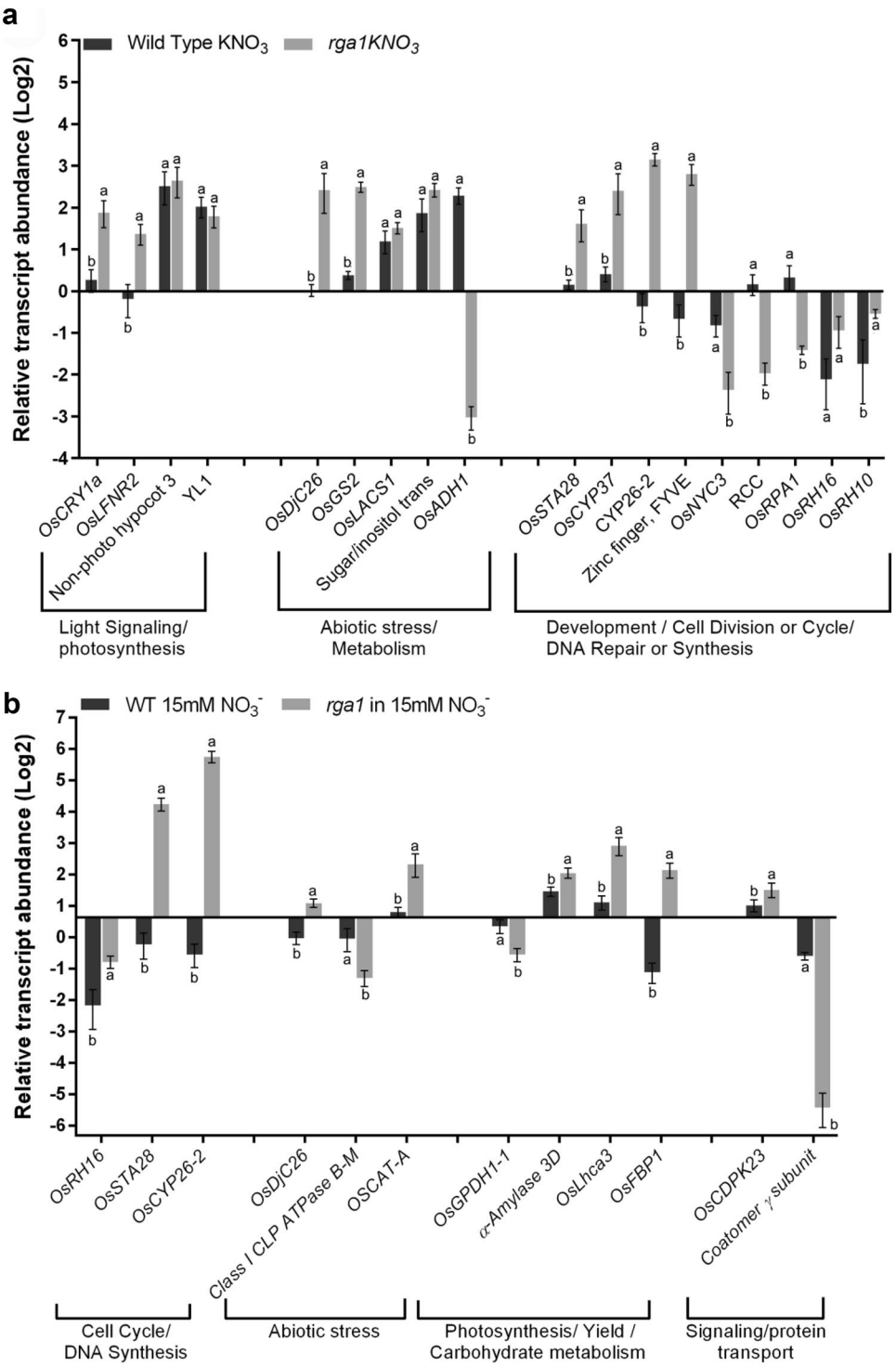

Fig. 5 Validation of expression profile of selected novel nitrate-responsive DEGs in the *rga1* mutant (*d1*) vs the corresponding WT by RT-qPCR. **a** RNA from excised leaves of 32-day-old rice seedlings treated in vitro with control (120 mM KCl) and nitrate (120 mM KNO_3) and **b** RNA from leaves of potted intact plants at active tillering stage, treated in vivo by growing them throughout with AH nutrient solution containing 1.5 mM (control) or 15 mM nitrate. Relative change in the gene expression was calculated by comparative Ct method and actin genes were used for data normalization. The control values were taken as zero and only the test values are shown as averages of three technical and three independent biological replicates (±SE). The statistical significance is calculated using one-way ANOVA in GraphPad Prism 6.0 and same letters denote non-significant pairs. Log2Fold change values for the DEGs using RT-qPCR and microarray data showed a positive correlation of >83% (Supplementary Table 10)

RGA1 regulation for novel genes and processes for subtle N-responsive effects in the mutant. On the basis of literature (Kumari et al. 2021; Neeraja et al. 2021; Sandhu et al. 2021), we report 226 NUE-related DEGs (compared to 477 in WT) in the mutant using the nitrate-responsive transcriptome (Supplementary Fig. 8 and Supplementary Table 11). We validated the nitrate-responsive expression of six upregulated (*OsCRY1a*, *OsLFNR2*, *YL1*, *OsGS2*, *OsFBP1* and *α-amylase 3D*) and three downregulated (*OsADH1*, *OsNYC3* and *OsRH10*) NUE-related DEGs (Fig. 5).

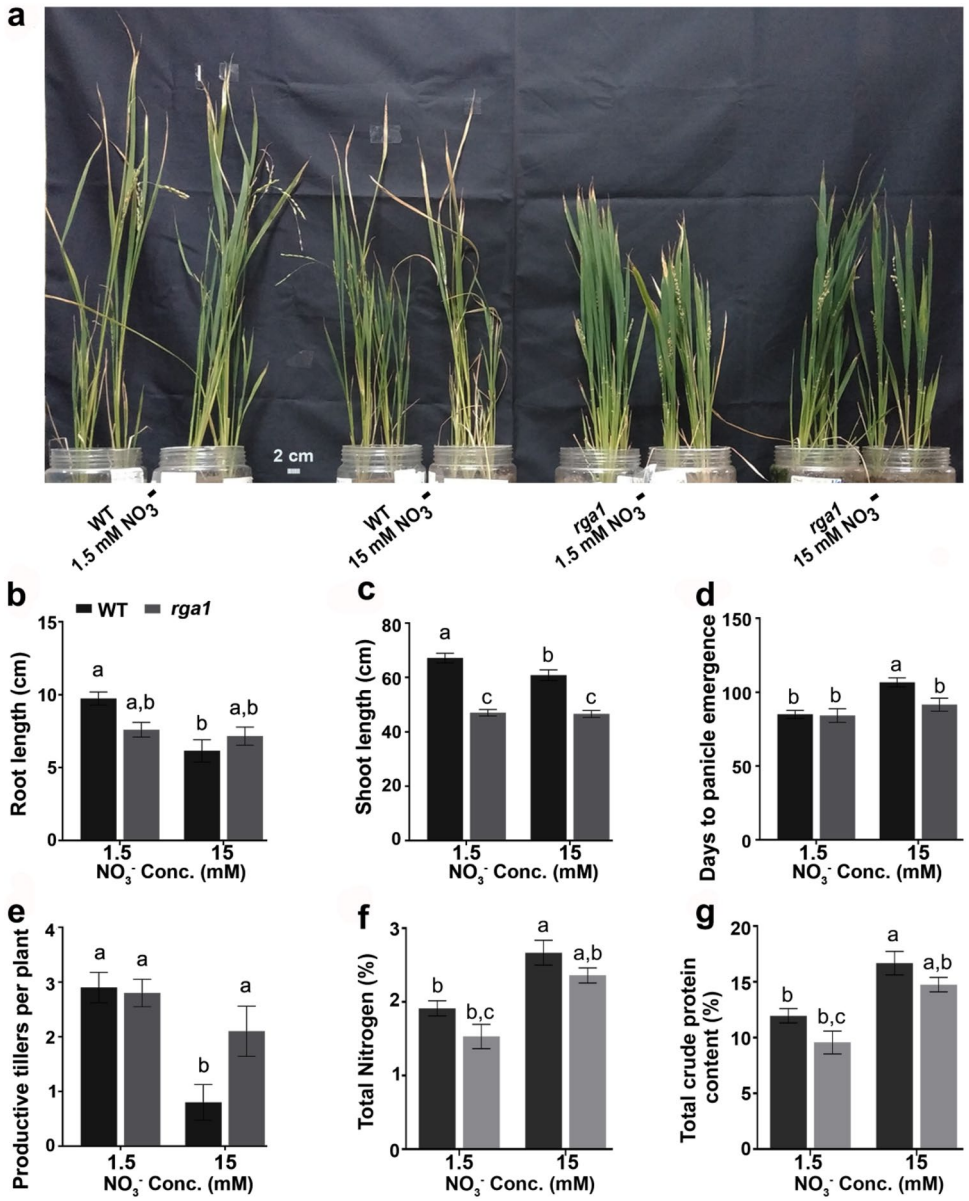

Fig. 6 Phenotypic measurements of rice WT and *rga1* mutant (*d1*) in response to two different doses of nitrate. **a** Representative image of WT and *rga1* mutant plants grown in pots with two different concentrations of nitrate. **b** Bar graph showing the root length of 20-day-old seedlings grown hydroponically at two different nitrate concentrations. **c** Bar graph representing the shoot length of WT and *rga1* mutant plants at heading stage grown in pots with two different concentrations of nitrate. **d** Bar graph representing the days to panicle emergence in WT and *rga1* mutant plants grown in pots with two different concentrations of nitrate. **e** Bar graph representing the number of productive tillers in WT and *rga1* mutant plants grown in pots with two different concentrations of nitrate. **f** Bar graph representing the total N content per plant in WT and *rga1* mutant plants grown in pots with two different concentrations of nitrate. **g** Bar graph representing the total protein content per plant in WT and *rga1* mutant plants grown in pots with two different concentrations of nitrate. **b**-**e** Each bar graph represents mean ± SE of the data from twelve biological replicates. **f**, **g** Each bar graph represents mean ± SE of the data from three independent biological replicates. The statistical significance is calculated using two-way ANOVA in GraphPad Prism 6.0 and same letters denote non-significant pairs

Phenotypic and physiological validation of differential N-response in mutant and WT

Phenotypic data were generated using the same plants used for RT-qPCR validation of DEGs associated with agronomic traits (Fig. 5b), to relate gene expression found in leaves to other organs, traits and overall comparative agronomic performance in WT and mutant plants. For this purpose, 10-day-old seedlings were grown hydroponically in AH solution containing either 1.5 or 15 mM nitrate for next

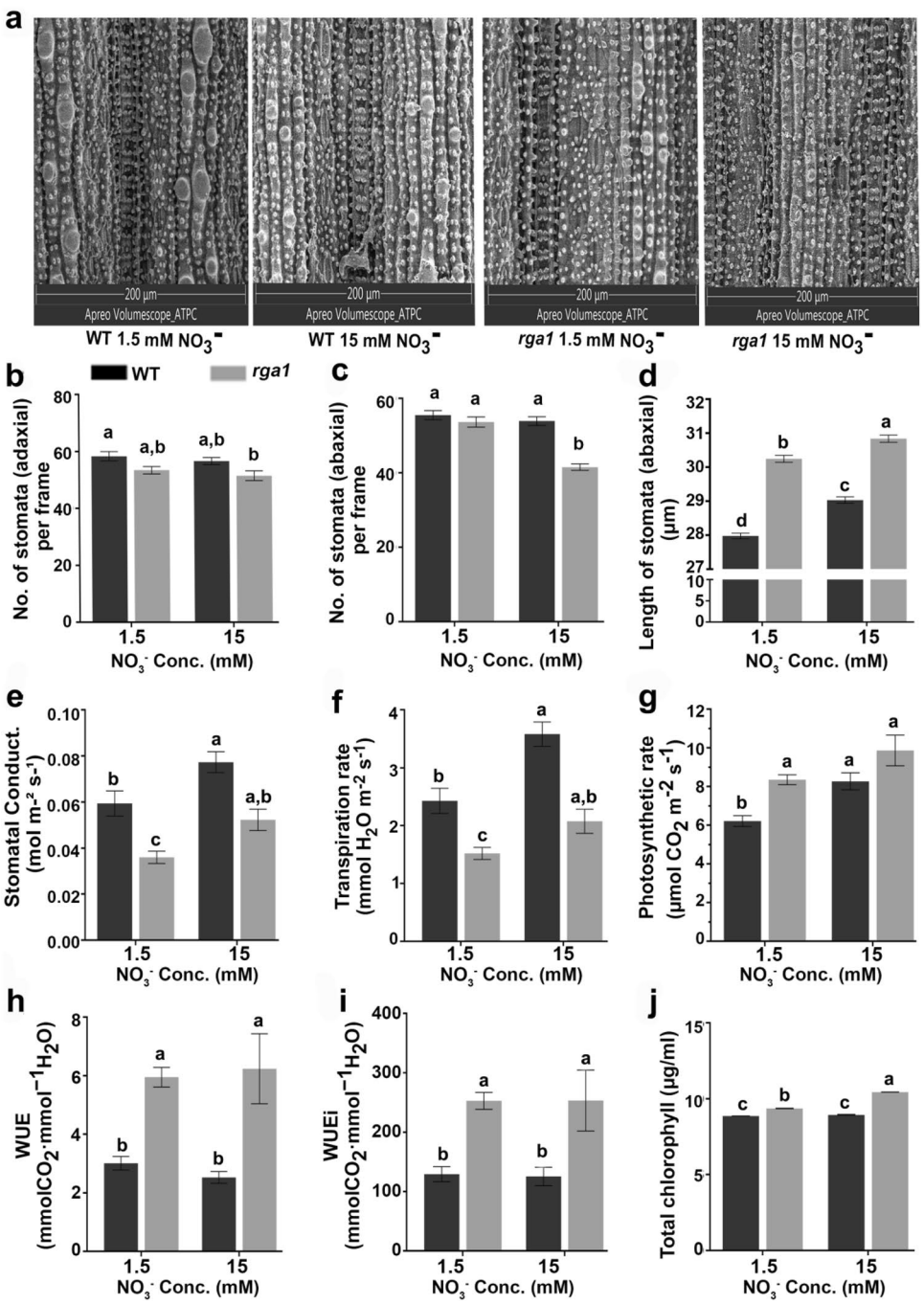

Fig. 7 Physiological measurements of rice WT and *rga1* mutant (*d1*) in response to two different doses of nitrate (1.5 mM or 15 mM) at early vegetative stage. Measurements of stomatal density and physiology of rice WT and the mutant in response to two different doses of nitrate. Stomatal density on **a**, **b** the adaxial leaf surfaces and **c** abaxial surface. **d** Stomatal size on the abaxial surface. Measurement of **e** stomatal conductance, **f** transpiration rate, **g** photosynthetic rates, **h** water use efficiency (photosynthetic rate/transpiration rate), **i** intrinsic water use efficiency (photosynthetic rate/stomatal conductance) of photosynthetically active fully developed leaf at active tillering stage. Measurement of **j** total chlorophyll content of photosynthetically active fully developed leaf at active tillering stage. SEM analyses were performed using three independent biological replicate plants and two technical replicates from each plant. Stomatal density was analyzed in frames of 550.56 × 825.43 (H × W) μm^2 area on the leaf surfaces. **e**–**i** Bar graphs represent mean ± SE of the data from five independent biological replicate plants. **j** Bar graphs represent mean ± SE of the data from three independent biological replicate plants. The statistical significance is calculated using two-way ANOVA in GraphPad Prism 6.0 and same letters denote non-significant pairs

10 days and then their root lengths were recorded (Fig. 7b). Under the contrasting doses of nitrate, WT and mutant plants exhibited significant differences in phenotypic and physiological responses in four independent experiments (Figs. 6, 7, 8 and Supplementary Figs. 9, 11, 12). The duration of treatments was selected based on our previous experiments with WT *japonica* plants, wherein significant N-dose-responsive phenotypic and physiological differences were observed with 20 days old seedlings and thereafter throughout the life cycle (Mandal et al. 2022). Root lengths were significantly longer, as expected in the WT plants treated with 1.5 mM NO_3^- relative to 15 mM. However, no significant difference in root length was observed in mutant plants under any nitrate concentration (Fig. 6b). The same trend was also observed for shoot length (Fig. 6c). Similarly heading date and productive tillers were affected by 15 mM NO_3^- (relative to low N) in the WT but not in the mutant (Fig. 6 d,e). These consistent results across multiple growth and yield-related parameters suggest that the mutation in *RGA1* may have rendered the plant insensitive to changes in

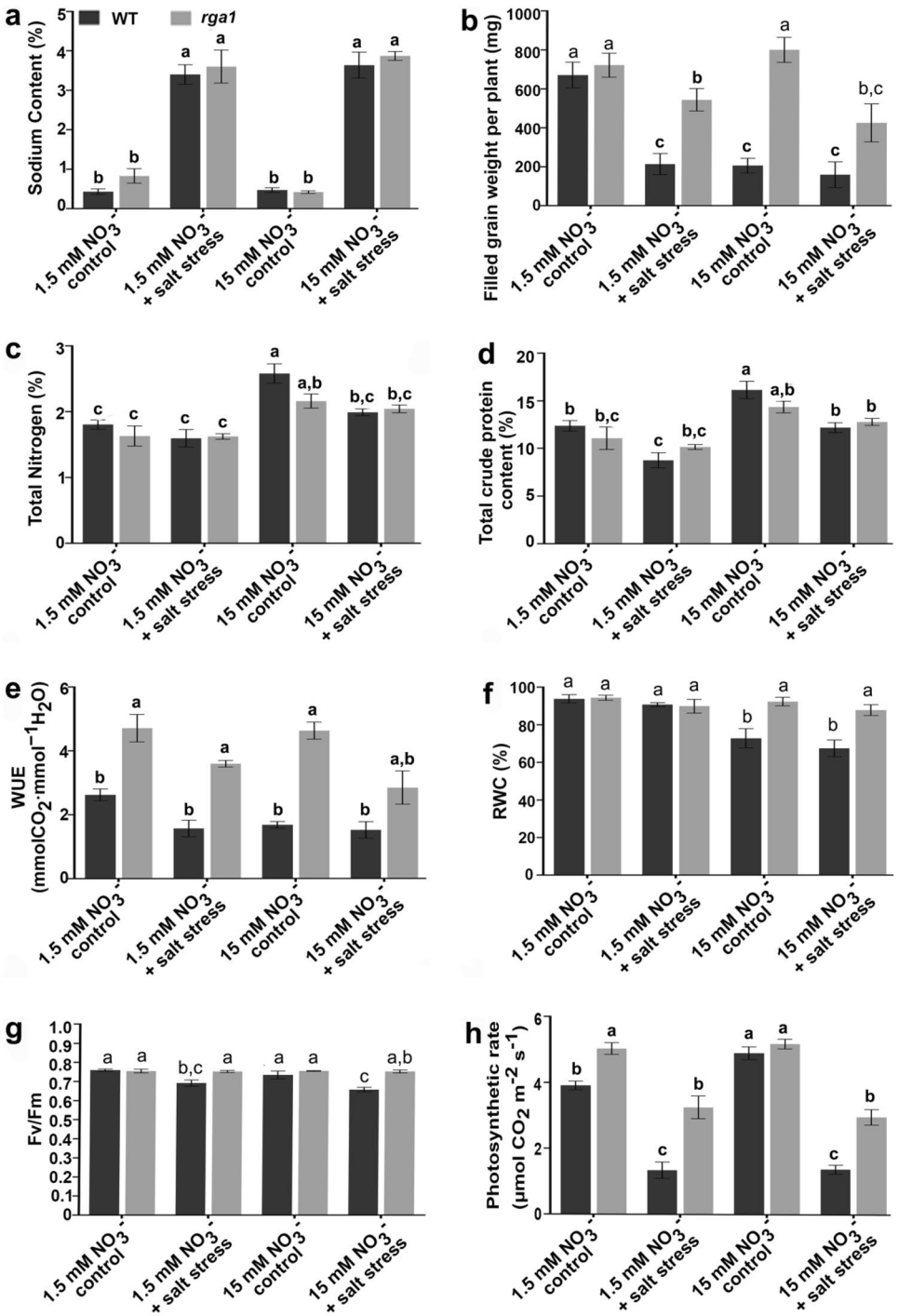

Fig. 8 Physiological measurements of rice WT and *rga1* mutant (*d1*) in response to two different doses of nitrate (1.5 mM or 15 mM) and salt stress during grain filling stage. Measurements of sodium content (**a**), total filled grain weight per plant (**b**), nitrogen content (**c**) and protein content (**d**) in rice WT and the mutant plants at harvest in response to two different doses of nitrate with or without salt stress. Measurement of water use efficiency (photosynthetic rate/transpiration rate) (**e**), relative water content (**f**), Fv/Fm; maximal quantum efficiency of photosystem II (PSII) (**g**) and photosynthetic rates (**h**) of photosynthetically active leaf (**h**) of rice WT and the mutant plants in response to two different doses of nitrate with or without salt stress salt stress. Bar graphs **b**, **e**–**h** represent mean ± SE of the data from at least six independent biological replicate plants. Bar graphs **a**, **c**, **d** represent mean ± SE of the data from at least four independent biological replicate plants. The statistical significance is calculated using three-way ANOVA in GraphPad Prism 6.0 and same letters denote non-significant pairs

N-supply/content, which may explain its better NUE relative to WT, especially at 15 mM NO_3^- (Fig. 1b, c).

Total nitrogen and total protein contents were found to be higher in 15 mM NO_3^- treated plants as compared to the 1.5 mM NO_3^- treated ones in both the WT and mutant plants. However, the mutants had lower total nitrogen and total protein contents relative to the WT (Fig. 6f,g). Our measurements of relative water content and catalase activity (Supplementary Fig. 9) in these plants indicate higher N-dose sensitivity in WT at 15 mM NO_3^- as compared to the mutant. Similarly, our data shown in Supplementary Fig. 10 show insignificant differences in P contents at the harvest stage, though the differences in K content between WT and mutant were significant only at 1.5 mM nitrate and not at 15 mM nitrate.

To reconfirm that the phenotypic results are solely due to N-response and not any other external effect, we repeated the experiment with higher light intensity (200 µmol m^{-2} s^{-1}) at the plant level in the growth chamber. We also saturated

the pots with water to rule out any water deficiency and still obtained similar N-responsive results. Our data in Supplementary Fig. 12 show that *RGA1* mutant was insensitive to N-dose while the WT exhibited N-dose sensitivity and decreased plant height. Further, we showed here that *RGA1* mutation renders even other agronomically important traits unaffected by N-dose (Fig. 6). Consequently, the inhibition of yield and NUE seen in the WT at 15 mM nitrate did not manifest in the mutant, thus appearing to perform better in terms of yield and NUE-related parameters.

The total number of stomata on leaf surfaces did not show any significant difference attributable to nitrate dose in the wild type plants, however, it was lower in the mutant plants at 15 mM NO_3^- relative to 1.5 mM nitrate (Fig. 7a–c). On the other hand, significant effect of nitrate dose was observed in the stomatal length on the abaxial surfaces of both WT and mutant leaves (Fig. 7d). Moreover, the mutant plants showed larger stomata relative to the WT, as is known in Arabidopsis (Zhang et al. 2008) but not reported for N-response in rice so far to our knowledge. Stomatal conductance and transpiration rate increased with increase in nitrate concentration in the WT plants; while the mutant did not show significant change with respect to N-dose (Fig. 7e, f). However, the mutant plants exhibited lower stomatal conductance and transpiration rates relative to the WT irrespective of the N-dose.

Interestingly, the mutant plants also showed significantly higher chlorophyll content than their corresponding WT irrespective of the nitrate concentration, with visibly darker green leaves of the mutant plants (Fig. 7j). Nitrate dose had significant effect on the chlorophyll content only in mutant plants, as those grown under 15 mM NO_3^- had significantly higher chlorophyll content than those grown under 1.5 mM NO_3^- (Fig. 7j). However, nitrate concentration did not significantly affect the photosynthetic rate in the mutants, whereas a significant increase was observed in case of WT plants from 1.5 mM to 15 mM nitrate concentration at both early (Fig. 7g) and late vegetative stages (Supplementary Fig. 11). Additionally, mutant plants showed better water use efficiency (WUE) and intrinsic water use efficiency (WUEi) owing to higher photosynthetic rate and lower stomatal conductance and transpiration rates (Fig. 7h, i and Supplementary Fig. 11).

Abiotic stress tolerance/resistance is one of the best studied roles of *RGA1*. It also emerged as an important process in the functional annotation of the DEGs in WT and *RGA1* to nitrate in this study (Fig. 4). Further physiological examination was done on the effect of nitrate dose (1.5 and 15 mM nitrate) and/or salt stress (120 mM NaCl) on grain yield in the WT and *RGA1* mutant. It revealed that despite similar sodium accumulation, the mutant was far less sensitive (or far more tolerant) to both nitrate dose and salt (Fig. 8a, b). However, the lack of additive effect of higher nitrate/salt on yield in the WT as well as in the mutant indicates that nitrate and salt affect yield through the same regulatory step. In other words, *RGA1* emerges as a convergence point in the mechanism of salt tolerance and NUE for the first time.

The total nitrogen content in the shoot increased from 1.5 to 15 mM nitrate in both the WT in the mutant, though to a slightly lesser degree in the mutant than in the WT (Fig. 8c). This explains why the mutant is less sensitive to the inhibitory effects of nitrate dose on root/shoot length and yield than the WT and suggests that *RGA1* regulate nitrate uptake. Interestingly, the same cannot be said for reduced sensitivity to salt stress in the mutant, as the sodium content remained unchanged between the WT and mutant (Fig. 8a). Total protein contents increased in response to N-dose in both WT and the mutant, but were more affected by salt stress in the WT and non-significantly in the mutant (Fig. 8d). Interestingly, this is not due to reduced sodium intake in the mutant and is inspite of the reduced nitrogen content in the mutant (Fig. 8a) and needs further exploration for other mechanisms. *RGA1* mutant plants also showed lower physiological sensitivity than WT to salt stress at both the N doses and maintained better maximal quantum efficiency of photosystem II (Fv/Fm) photosynthetic rate, water use efficiency and relative water content (Fig. 8e–h).

Overall, these findings on nitrate-responsive phenotypic traits must have a basis in differential gene expression in the mutant plants, as many of the nitrate-responsive DEGs found in this study are functionally linked to such phenotypic traits (Fig. 4, Supplementary Figs. 5, 6 & 13). The lesser number of DEGs with higher foldchange in mutant over WT may be due to the reduced N-sensitivity of the mutant relative to the WT, which may in turn subdue the associated phenotypic effects. PPI network of total DEGs in the mutant for traits like leaf and/or culm and/or root, panicle and/or seed and/or yield and tolerance and/or resistance were mainly enriched with upregulated DEGs (Fig. 9). At least 14 of them have been validated as nitrate responsive by RT-qPCR (Fig. 5), clearly indicating their role in regulating the agronomic response to nitrate through G-protein (*RGA1*) signalling in rice. They are *OsGS*2, *OsLFNR2*, *OsADH1*, *YL1*, *OsNYC3*, *OsSTA28*, *Oslhca3*, *OsCAT-A*, *Regulator of chromosome condensation*, *OsRH16*, *OsFBP1, OsRH10*, *Class I CLP ATPase B-M* and *Catomer γ subunit.*

Discussion

Our earlier transcriptomic studies on G-protein α subunit mutants identified differential expression of some genes involved in N-response/metabolism in *Arabidopsis* (Chakraborty et al. 2019; Chakraborty et al. 2015a, b, c) and rice (Pathak et al. 2021). But a thorough validation of the role of Gα in genomewide nitrate response was long

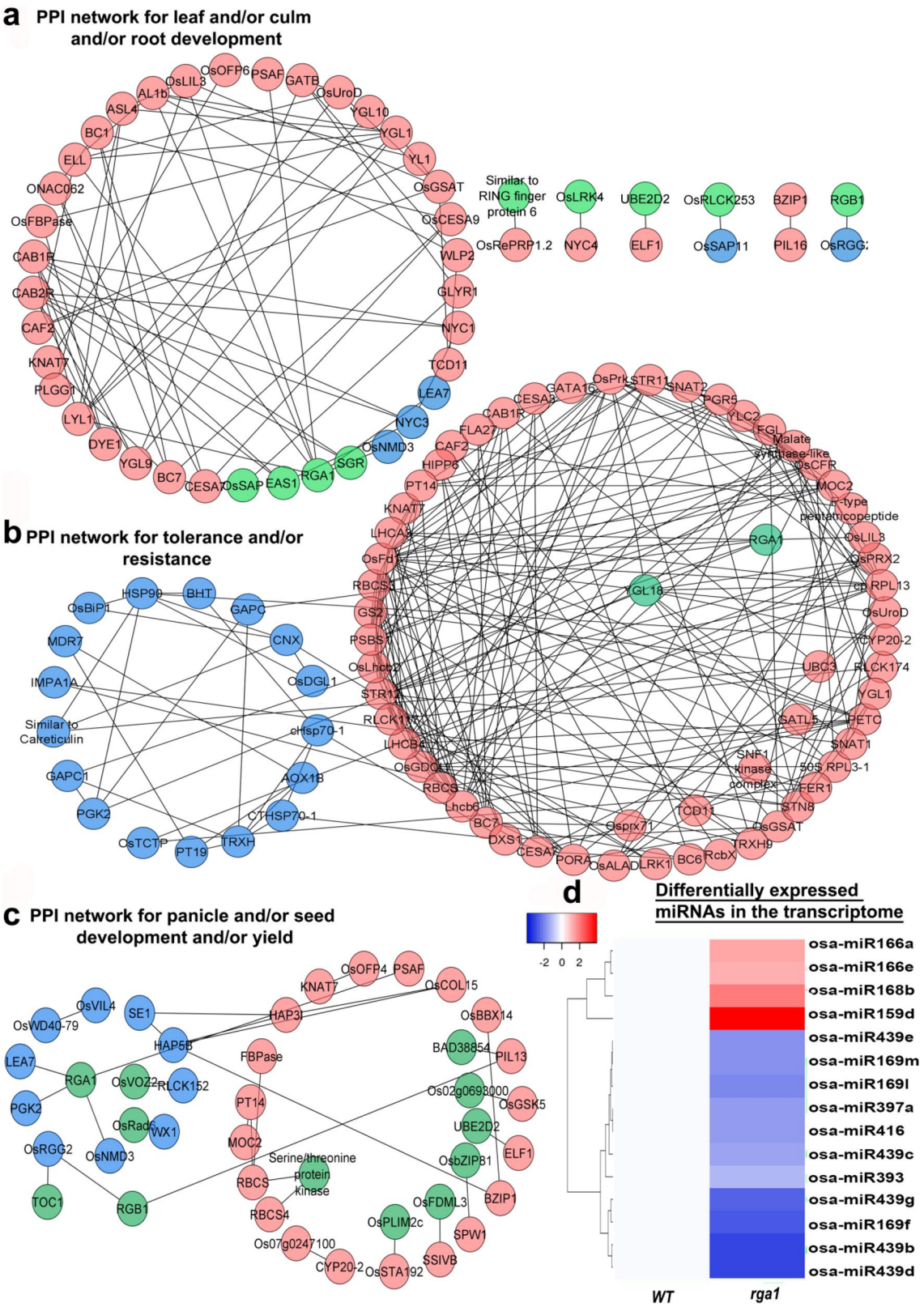

Fig. 9 Protein–protein interaction network of DEGs involved in regulation of plant traits. **a** Leaf and/or culm and/or root development, **b** tolerance and/or resistance and **c** panicle and/or seed development and/or yield. **d** Heatmap depicting expression levels of differentially regulated miRNAs in *rga1* mutant (*d1*) mutant in response to nitrate. The nodes in red and blue colour represent the up- and downregulated nitrate-responsive DEGs, respectively, some of which are validated by RT-qPCR. Interactors that are not DEGs are shown in green colour

overdue, especially in view of its agronomic implications in crop plants and the availability of the rice *d1* mutant devoid of functional Gα (*RGA1*).

The present study was prompted by the meta-analyses that revealed significant overlaps between N-responsive genes and *RGA1*-regulated genes, as well as better yield and NUE in the mutant relative to WT under 15 mM Nitrate treatment (Fig. 1a–c). While further exploitation of the NUE trait in the natural *RGA1* mutant can be taken up through agronomic field trials, we sought to understand its functional biology. It was specifically designed to examine the transcriptome-wide N-response in the *rga1* mutant and to compare it with its corresponding WT nitrate-responsive transcriptome generated simultaneously under identical conditions (Mandal et al. 2022). We identified the common and many exclusive DEGs/pathways/processes in the mutant and WT for the associated NUE-related phenotypic and physiological aspects for a more comprehensive understanding. To the best of our knowledge, this is the first attempt to address most of the published rice NUE traits together in the *RGA1* mutant with two N doses and represents a convergence of two long tracks of work (Raghuram 2023).

N-responsive genes/processes in *RGA1* mutant

A proper characterization of the effect of *RGA1* mutation on genomewide N-response would require baseline knowledge of nitrate response in the corresponding WT. Our earlier studies on nitrate response were carried out in *indica* background to search for candidate target genes to improve NUE in rice (Pathak et al. 2020; Sharma et al. 2022). We recently generated similar genomewide nitrate-response data in *japonica* using KCl as a control for KNO_3 and reported 6688 DEGs (Mandal et al. 2022). In view of several overlapping genes between nitrate-response and *RGA1*-response, we analyzed the effect of *RGA1* mutation on the genomewide nitrate response in the present study. The raw data are provided at NCBI GEO database (GSE62164). We hereby report 3416 DEGs and their associated processes, traits etc., and also compare it with the corresponding WT DEGs.

These 3416 nitrate-responsive genes we identified in the mutant for the first time are larger in number than those regulated by *RGA1*-alone (Figs. 1a, 2a) and only 605 of them are in common with Ferrero-Serrano et al. (2018) and 474 common with Pathak et al. (2021). Venn comparison with all the nitrate-responsive DEGs found in WT under identical conditions revealed 1749 unique DEGs in the mutant, apart from those common (1667) and exclusive in the WT (5021; Fig. 2b, c). We found opposite trend of expression between the mutant and WT in 28 upregulated and 30 downregulated DEGs, some of which were validated by RT-qPCR (Fig. 5). This could mean that the Gα knock-out mutation has reversed the nitrate-response for these genes, but this does not seem to have any measurable impact on the growth parameters, which seem to be insensitive to N-supply or N-dose in the mutant (Figs. 6, 7, 8). Some degree of insensitivity can be explained with our transcriptomic data that lesser number of DEGs (related to various N-responsive traits) with higher foldchange were enriched in the mutant than WT (Fig. 4).

Though nitrate upregulated most of the genes for increased photosynthesis both in WT as well as mutant plants, their proportion was higher in the mutant (68 out of 72 or 94%) as compared to 73% in WT. This is consistent with our finding that chlorophyll biosynthetic/metabolic process was significantly enriched for upregulated DEGs only in mutant. These results are in line with some earlier reports on the role of G-proteins in better light harvesting (Ferrero-Serrano et al. 2018) and photosynthesis in Arabidopsis (Zhao et al. 2010) and rice (Wang et al. 2021) but reported in nitrogen response for first time in the current study. Our results add N-responsive DEGs to the earlier reported biological processes in the mutant that include cell redox homeostasis (Yadav et al. 2013; Chakraborty et al. 2015a, b, c; Swain et al. 2017), regulation of ARF protein signal transduction (Donaldson et al. 1991) and cellular protein metabolism.

Among the DEGs hitherto unknown to be both *RGA1*-regulated and N-responsive, there are those belonging to several regulatory classes like TFs, RLKs, MAP Kinases, hormones and G-proteins and calcium signalling with agronomic influence, as elaborated below.

Association of DEGs with phenotypic/agronomic traits

Out of 1323 N-responsive DEGs associated with important phenotypic/agronomic traits in the WT (Mandal et al. 2022), only 719 were nitrate-responsive in the mutant. But there were 381 others that responded to nitrate only in the mutant and not in the WT, whereas reverse was true for 985 DEGs (Supplementary Table 7). Only 151 of these DEGs were found in the mutant transcriptome by Ferrero-Serrano et al. (2018), without reference to nitrate or any agronomic trait. Similarly, 186 such DEGs were found in the mutant transcriptome by Pathak et al. (2021), with some reference to agronomic traits and annotations associated with nitrate metabolism. The identification of over 3.6-fold more DEGs associated with N-response and Gα-regulated phenotypic/agronomic traits in this study indicates the importance of experimentally examining nitrate response in the mutant. The lesser number of highly up- or downregulated phenotypic trait-related DEGs in the mutant (relative to the WT) may account for the different phenotypic and physiological responses in the mutant (Figs. 6, 7, 8 and Supplementary Table 7).

The mutant was not sensitive to N-dose (15 mM) relative to the WT with respect to growth parameters such as root/shoot length, number of productive tillers, heading date/panicle emergence and yield (Fig. 6 and Supplementary Figs. 9 & 12). This insensitivity seems to translate into better NUE in the mutant as compared to the WT (Fig. 1c), especially at 15 mM relative to 1.5 mM NO_3^-. However, both the mutant and WT displayed significant N-dose responsive changes in stomata, photosynthesis, chlorophyll, total N and protein contents (Figs. 7, 8 and Supplementary Fig. 11). RT-qPCR validation of DEGs (Fig. 5) encompassing diverse functional categories indicated links between N- and *RGA1*-mediated regulation of several agronomic traits as discussed below.

The N-dose insensitivity of root and shoot growth in the mutant (Fig. 6a, b and Supplementary Figs. 9 & 12) may be explained in part by the predominance of lower fold change (1–2) DEGs and the reduced number of higher foldchange (3–8) DEGs as compared to the WT (Supplementary Table 7 and Supplementary Fig. 13). These findings were further strengthened by the upregulated DEGs and their experimentally validated interactions, which were predominant in the mutant (Fig. 9) relative to the corresponding WT (Mandal et al. 2022). Our RT-qPCR validation of downregulation of *OsNYC3* (LOC_Os06g24730, *NON-YELLOW COLORING 3*) (Fig. 5), which is involved in chlorophyll degradation can explain the N-responsive increase of chlorophyll content in the mutant (Cao et al. 2022). Further, the preponderance of uniquely upregulated DEGs belonging to photosynthesis, light harvesting and chlorophyll biosynthesis (five of which were validated by RT-qPCR) in the mutant may explain its better photosynthetic capacity than WT irrespective of N-dose (Figs. 5, 7g). Better NUE at 15 mM N for the mutant can also be explained by such improved photosynthetic and stomatal response as well as WUE (Fig. 7h, i and Supplementary Fig. 11) together with upregulation of many NUE-related DEGs belonging to light signalling and/or photosynthesis (5 such validated in Fig. 5; *OsCRY1a*, *OsLFNR2, YL1, OsFBP1* and *α-amylase 3D*). Interestingly, yield and number of productive tillers per plant were also insensitive or non-responsive to nitrate dose in the mutant, whereas both declined in the WT from 1.5 to 15 mM nitrate (Figs. 1b, 6e). This could be because nitrate-dose sensitivity inhibited yield in the WT at 15 mM (relative to 1.5 mM), but not in the mutant (Fig. 1b, c). Our physiological validation of nitrate-response in the WT showed reduced water use efficiency owing to increased stomatal conductance and transpiration (Fig. 7). Also, Fv/Fm; maximal quantum efficiency of photosystem II (PSII), relative water content (Fig. 8f, g) and catalase activity (Supplementary Fig. 9) were reduced in the WT plants at 15 mM N, but not in the mutant (with or without 120 mM salt stress). These differences corresponded with the higher proportion of upregulated DEGs related to traits like seed development, yield and tolerance and/or resistance in the mutant transcriptome but greater number of highly up- and downregulated DEGs in the WT (Supplementary Table 7). Most of the DEGs belonged to lower foldchange in the mutant. This was validated by RT-qPCR with the upregulation of NUE-related *OsFBP1* (LOC_Os01g64660) and *ALPHA-AMYLASE 3D* (LOC_Os08g36910) in whole plant leaves (Fig. 5b). These genes are known to be related to seed development and/or yield (Damaris et al. 2019).

We also validated four upregulated (*OsDjC26*, *OsCAT-A, OsLACS1, Sugar/inositol transporter*) and three downregulated DEGs in the mutant related to tolerance and/or resistance by RT-qPCR (Fig. 5). They include *OsRH10* (LOC_Os03g46610) and *OsRH16* (LOC_Os03g51900), related to tolerance and growth at higher temperatures (Wang et al. 2016) that were less severely downregulated in the mutant than the WT. These results indicate the role of Gα as a common link between abiotic stress and nitrate response, an under explored area (Jangam and Raghuram 2015). Our current physiological data strengthen this link, as the *RGA1* mutation significantly reduced the impacts of nitrate dose and salt stress on grain yield, comparably but non-additively (Fig. 8b). The mutant plants also exhibited lesser impact of salt stress on protein content at higher nitrate dose at the grain filling stage (Fig. 8c, d). Overall, *RGA1* mutant plants showed lower physiological sensitivity than WT to salt stress at both the N doses and protected their photosynthetic performance, water use efficiency, relative water content (Fig. 8e–h). The improved stress tolerance of the *RGA1* mutant is also evidenced by the upregulation of *OsCAT-A* gene expression (Fig. 5b) and catalase activity at 15 mM NO_3^- than the WT (Supplementary Fig. 9).

Such changes in the gene expression are in line with earlier reports on the role of G-protein signalling in improving tolerance to abiotic and biotic stresses (Chakraborty et al. 2015a, b, c; Ferrero-Serrano et al. 2018; Jangam et al. 2016; Kaur et al. 2018; Urano et al. 2020; Zait et al. 2021). One possible mechanism for such tolerance could be through higher photosynthesis and lower transpiration displayed by the mutant, apart from higher WUE owing to less stomatal density (Fig. 7). This is in line with earlier reports of higher photosynthates in mutants of *AGB1* in *Arabidopsis* (Mudgil et al. 2016). Our RT-qPCR validated the nitrate upregulation of four genes viz. *OsFBP1*, *ALPHA-AMYLASE 3D*, *OsCDPK23* and *OsLhca3* in whole plant leaves and *OsLFNR2* related to photosynthesis and/or carbohydrate metabolism in excised leaves. Further, the validated upregulation of *OsGS2* (chloroplastic glutamine

synthetase, LOC_Os04g56400) and *YELLOW-LEAF 1* (LOC_Os01g17170) related to N metabolism in the mutant may account for increased total N and protein content at 15 mM NO_3^-, despite N insensitive phenotypic growth. Finally, a total of 53 genes encoding proteins for light harvesting complex or photosystem I and II were enriched in our data, which is in line with similar results obtained for Arabidopsis (Warpeha et al. 2006, 2007). Most of these genes were upregulated and some of them were validated (Fig. 5). Therefore, higher rate of photosynthesis along with better stomatal physiology (Ferrero-Serrano et al. 2018) may account for better yield in the *rga1* mutant relative to the wild type. This indicates that G-protein signalling may regulate tolerance towards nitrate dose and NUE, much the same way as it might regulate salt stress tolerance.

Conclusion

The current study used genomewide nitrate-response of a knock-out mutant of the G-protein α subunit (*RGA1*) in *japonica* rice to show that it regulates N-dose-sensitivity in some N-responsive parameters that contribute to yield and NUE. Our nitrate-responsive microarray analyses revealed many novel *RGA1*-regulated genes/processes involved in NUE. We identified their phenotypic association with root/shoot, stomata, tiller, panicle/flowering and yield, with better chlorophyll content and photosynthesis, transpiration rate and stomatal density/conductance and better water use efficiency and salt tolerance as important for NUE. Overall, our integration of the genomewide nitrate-responsive transcriptome analysis with its physiological and phenotypic underpinnings provide clinching genetic evidence to show that Gα could be an important link between G-protein signalling and NUE. This opens up many opportunities for further studies to understand the underlying mechanisms, as well as to use it for the improvement of NUE.

Supplementary Information The online version contains supplementary material available at https://doi.org/10.1007/s00299-023-03078-7.

Acknowledgements We thank Prof. T. Kumamaru from Kyushu University for providing the rice seeds and Regional Centre for Biotechnology (RCB), Faridabad for their help with the scanning electron microscopy.

Author contributions JAP: planned the experiment, performed the microarray. VKM: performed the phenotypic, physiological, biochemical and qPCR validation. Performed part of in-silico analysis of microarray data. Assisted in writing and finalizing the draft of the manuscript. NC: performed most of the *in-silico* analysis of the microarray data, assisted in performing the phenotypic, physiological and qPCR validation. Wrote the initial draft of the manuscript. DK: Planned and supervised the experiments for total nitrogen and protein contents. NR: conceived, planned and supervised the transcriptome analyses, data interpretation, edited and finalized the manuscript. All authors have reviewed the manuscript.

Funding This work was supported by research grants to NR from DST-SERB (F. No. CRG/2021/007467), ICAR (F. No. 2-2(60)/10-11/NICRA), Department of Biotechnology (DBT) [BT/IN/UK-VNC/44/NR/2015-16], UKRI GCRF South Asian Nitrogen Hub (SANH) [NE/S009019/1], GGSIPU[GGSIPU/DRC/Ph.D/Adm/2016/1549], [GGSIPU/DRC/FRGS/2018/22] and [GGSIPU/DRC/FRGS/2019/1553/24]. Fellowships were paid to VKM from DBT (DBT/JRF/14/AL/445) and GGSIPU (STRF: GGSIPU/DRC/2020/2049), APJ from CSIR (09/806(013)2008-EMR-I) and NC from UKRI GCRF-SANH [NE/S009019/1].

Data availability/accession numbers Our raw microarray data that support the findings of this study have been deposited in NCBI–GEO database (https://www.ncbi.nlm.nih.gov/geo/query/acc.cgi?acc=GSE62164) with the accession number GSE62164 (GSM1520728, GSM1520729, GSM1520733, GSM1520732, GSM1520736 and GSM1520737). Additional transcriptome datasets were obtained from either the published supplementary materials and/or their authors cited in the article. All other datasets pertaining to the analyses are included in the supplementary information files.

Declarations

Conflict of interest The authors declare no conflict of interest.

References

Abrol YP, Adhya TK, Aneja VP, Raghuram N, Pathak H, Kulshrestha U, Sharma C, Singh B (2017) The Indian nitrogen assessment: sources of reactive nitrogen, environmental and climate effects, management options, and policies. Elsevier, Amsterdam

Ali A, Sivakami S, Raghuram N (2007) Regulation of activity and transcript levels of NR in rice (*Oryza sativa*): roles of protein kinase and G-proteins. Plant Sci 172:406–413

Ashikari M, Wu J, Yano M, Sasaki T, Yoshimura A (1999) Rice gibberellin-insensitive dwarf mutant gene Dwarf 1 encodes the α-subunit of GTP-binding protein. Proc Natl Acad Sci 96:10284–10289

Bhatnagar N, Pandey S (2020) Heterotrimeric G-protein interactions are conserved despite regulatory element loss in some plants. Plant Physiol 184:1941–1954

Bloom AJ (2015) The increasing importance of distinguishing among plant nitrogen sources. Curr Opin Plant Biol 25:10–16

Boonburapong B, Buaboocha T (2007) Genome-wide identification and analyses of the rice calmodulin and related potential calcium sensor proteins. BMC Plant Biol 7:1–17

Cao W, Zhang H, Zhou Y, Zhao J, Lu S, Wang X, Chen X, Yuan L, Guan H, Wang G (2022) Suppressing chlorophyll degradation by silencing OsNYC3 improves rice resistance to *Rhizoctonia solani*, the causal agent of sheath blight. Plant Biotechnol. J. 20:335–349

Chakraborty N, Sharma P, Kanyuka K, Pathak RR, Choudhury D, Hooley R, Raghuram N (2015a) G-protein α-subunit (GPA1) regulates stress, nitrate and phosphate response, flavonoid biosynthesis, fruit/seed development and substantially shares GCR1 regulation in A. thaliana. Plant Mol Biol 89:559–576

Chakraborty N, Sharma P, Kanyuka K, Pathak RR, Choudhury D, Hooley RA, Raghuram N (2015b) Transcriptome analysis of Arabidopsis GCR1 mutant reveals its roles in stress, hormones, secondary metabolism and phosphate starvation. PLoS ONE 10:e0117819

Chakraborty N, Singh N, Kaur K, Raghuram N (2015c) G-protein signaling components GCR1 and GPA1 mediate responses to multiple abiotic stresses in Arabidopsis. Front Plant Sci 6:1000

Chakraborty N, Kanyuka K, Jaiswal DK, Kumar A, Arora V, Malik A, Gupta N, Hooley R, Raghuram N (2019) GCR1 and GPA1 coupling regulates nitrate, cell wall, immunity and light responses in Arabidopsis. Sci Rep 9:1–17

Choudhury SR, Pandey S (2016) Interaction of heterotrimeric G-protein components with receptor-like kinases in plants: an alternative to the established signaling paradigm? Mol Plant 9:1093–1095

Choudhury SR, Li M, Lee V, Nandety RS, Mysore KS, Pandey S (2020) Flexible functional interactions between G-protein subunits contribute to the specificity of plant responses. Plant J 102:207–221

Coneva V, Simopoulos C, Casaretto JA, El-Kereamy A, Guevara DR, Cohn J, Zhu T, Guo L, Alexander DC, Bi Y-M (2014) Metabolic and co-expression network-based analyses associated with nitrate response in rice. BMC Genomics 15:1–14

Chen M, Chen G, Di D, Kronzucker HJ, Shi W (2020) Higher nitrogen use efficiency (NUE) in hybrid "super rice" links to improved morphological and physiological traits in seedling roots. J. Plant Physiol. 251:153191

Chen Y, Liu Y, Ge J, Li R, Zhang R, Zhang Y, Huo Z, Xu K, Wei H, Dai Q (2022) Improved physiological and morphological traits of root synergistically enhanced salinity tolerance in rice under appropriate nitrogen application rate. Front Plant Sci 13:982637

Cui Y, Jiang N, Xu Z, Xu Q (2020) Heterotrimeric G protein are involved in the regulation of multiple agronomic traits and stress tolerance in rice. BMC Plant Biol 20:1–13

Damaris RN, Lin Z, Yang P, He D (2019) The rice alpha-amylase, conserved regulator of seed maturation and germination. Int. J. Mol. Sci. 20:450

Donaldson JG, Kahn RA, Lippincott-Schwartz J, Klausner RD (1991) Binding of ARF and β-COP to Golgi membranes: possible regulation by a trimeric G protein. Science 254:1197–1199

Ferrero-Serrano Á, Su Z, Assmann SM (2018) Illuminating the role of the Gα heterotrimeric G protein subunit, RGA1, in regulating photoprotection and photoavoidance in rice. Plant Cell Environ 41:451–468

Fredes I, Moreno S, Díaz FP, Gutiérrez RA (2019) Nitrate signaling and the control of Arabidopsis growth and development. Current Opin. Plant Biol. 47:112–118

Gao Y, Qi S, Wang Y (2022) Nitrate signaling and use efficiency in crops. Plant Commun. 100353

Gao L-L, Xue H-W (2012) Global analysis of expression profiles of rice receptor-like kinase genes. Mol Plant 5:143–153

Hoagland DR, Arnon DI (1950) The water-culture method for growing plants without soil, 2nd edn. Circular California Agricultural Experiment Station, p 347

Hooper CM, Castleden IR, Aryamanesh N, Jacoby RP, Millar AH (2016) Finding the subcellular location of barley, wheat, rice and maize proteins: the compendium of crop proteins with annotated locations (cropPAL). Plant Cell Physiol 57:e9–e9

Hou M, Yu M, Li Z, Ai Z, Chen J (2021) Molecular regulatory networks for improving nitrogen use efficiency in rice. Int J Mol Sci 22:9040

Jangam AP, Raghuram N (2015) Nitrogen and stress. In: Pandey G (ed) Elucidation of abiotic stress signaling in plants. Springer, New York, pp 323–339

Jangam AP, Pathak RR, Raghuram N (2016) Microarray analysis of rice d1 (RGA1) mutant reveals the potential role of G-protein alpha subunit in regulating multiple abiotic stresses such as drought, salinity, heat, and cold. Front Plant Sci 7:11

Jin J, Tian F, Yang D-C, Meng Y-Q, Kong L, Luo J, Gao G (2016) PlantTFDB 4.0: toward a central hub for transcription factors and regulatory interactions in plants. Nucleic Acids Res. gkw982

Javed T, Indu I, Singhal RK, Shabbir R, Shah AN, Kumar P, Jinger D, Dharmappa PM, Shad MA, Saha D (2022) Recent advances in agronomic and physio-molecular approaches for improving nitrogen use efficiency in crop plants. Front. Plant Sci. 13

Joung J-G, Corbett AM, Fellman SM, Tieman DM, Klee HJ, Giovannoni JJ, Fei Z (2009) Plant MetGenMAP: an integrative analysis system for plant systems biology. Plant Physiol 151:1758–1768

Krouk G, Mirowski P, LeCun Y, Shasha DE, Coruzzi GM (2010) Predictive network modeling of the high-resolution dynamic plant transcriptome in response to nitrate. Genome Biol. 11:1–19

Kaur J, Roy Choudhury S, Vijayakumar A, Hovis L, Rhodes Z, Polzin R, Blumenthal D, Pandey S (2018) Arabidopsis type III Gγ Protein AGG3 is a positive regulator of yield and stress responses in the model monocot Setaria viridis. Front Plant Sci 9:109

Krapp A (2015) Plant nitrogen assimilation and its regulation: a complex puzzle with missing pieces. Curr Opin Plant Biol 25:115–122

Kronzucker HJ, Siddiqi MY, Glass AD, Kirk GJ (1999) Nitrate-ammonium synergism in rice. A subcellular flux analysis. Plant Physiol 119:1041–1046

Kanehisa M, Goto S (2000) KEGG: kyoto encyclopedia of genes and genomes. Nucleic Acids Res. 28:27–30

Kumari S, Sharma N, Raghuram N (2021) Meta-analysis of yield-related and N-responsive genes reveals chromosomal hotspots, key processes and candidate genes for nitrogen-use efficiency in rice. Front Plant Sci. https://doi.org/10.3389/fpls.2021.627955

Lichtenthaler H (1987) Chlorophyll and carotenoids–pigments of photosynthetic biomembrances za Colowick SP, Kaplan NO Methods in Enzymology. Vol. 148. In. Academic Press, San Diego

Li H, Hu B, Chu C (2017) Nitrogen use efficiency in crops: lessons from Arabidopsis and rice. J Exp Bot 68:2477–2488

Liang Y, Zhao X, Jones AM, Gao Y (2018) G proteins sculp root architecture in response to nitrogen in rice and Arabidopsis. Plant Sci 274:129–136

Loreto F, Velikova V (2001) Isoprene produced by leaves protects the photosynthetic apparatus against ozone damage, quenches ozone products, and reduces lipid peroxidation of cellular membranes. Plant Physiol. 127:1781–1787

Madan B, Malik A, Raghuram N (2022) Crop nitrogen use efficiency for sustainable food security and climate change mitigation. In: Kumar V, Srivastava AK, Suprasanna P (eds) Plant nutrition and food security in the era of climate change. Elsevier, Amsterdam, pp 47–72

Majumdar P, Torres Rodríguez MD, Pandey S (2023) Role of heterotrimeric G-proteins in improving abiotic stress tolerance of crop plants. J Plant Growth Regul. https://doi.org/10.1007/s00344-023-10965-6

Mandal VK, Sharma N, Raghuram N (2018) Molecular targets for improvement of crop nitrogen use efficiency: current and emerging options. In: Shrawat A, Zayed A, Lightfoot D (eds) Engineering nitrogen utilization in crop plants. Springer, Chamberland, pp 77–93

Mandal VK, Jangam AP, Chakraborty N, Raghuram N (2022) Nitrate-responsive transcriptome analysis reveals additional genes/processes and associated traits viz. height, tillering, heading date, stomatal density and yield in japonica rice. Planta 255:1–19

Maruta N, Trusov Y, Jones AM, Botella JR (2021) Heterotrimeric G proteins in plants: canonical and atypical Gα subunits. Int J Mol Sci 22:11841

Misyura M, Guevara D, Subedi S, Hudson D, McNicholas PD, Colasanti J, Rothstein SJ (2014) Nitrogen limitation and high

density responses in rice suggest a role for ethylene under high density stress. BMC Genomics 15:1–14
Móring A, Hooda S, Raghuram N, Adhya TK, Ahmad A, Bandyopadhyay SK, Barsby T, Beig G, Bentley AR, Bhatia A (2021) Nitrogen challenges and opportunities for agricultural and environmental science in India. Front Sustain Food Syst. https://doi.org/10.3389/fsufs.2021.505347
Mudgil Y, Karve A, Teixeira PJ, Jiang K, Tunc-Ozdemir M, Jones AM (2016) Photosynthate regulation of the root system architecture mediated by the heterotrimeric G protein complex in Arabidopsis. Front Plant Sci 7:1255
Meng X, Wang X, Zhang Z, Xiong S, Wei Y, Guo J, Zhang J, Wang L, Ma X, Tegeder M (2021) Transcriptomic, proteomic, and physiological studies reveal key players in wheat nitrogen use efficiency under both high and low nitrogen supply. J. Exp. Bot. 72:4435–4456
Nazish T, Arshad M, Jan SU, Javaid A, Khan MH, Naeem MA, Baber M, Ali M (2021) Transporters and transcription factors gene families involved in improving nitrogen use efficiency (NUE) and assimilation in rice (Oryza sativa L.). Transgenic Res. 1-20
Neeraja CN, Barbadikar KM, Mangrauthia SK, Rao PR, Subrahmanayam D, Sundaram RM (2021) Genes for NUE in rice: a way forward for molecular breeding and genome editing. Plant Physiol Rep 26:587–599
O'Brien JA, Vega A, Bouguyon E, Krouk G, Gojon A, Coruzzi G, Gutiérrez RA (2016) Nitrate transport, sensing, and responses in plants. Mol Plant 9:837–856
Pandey S, Vijayakumar A (2018) Emerging themes in heterotrimeric G-protein signaling in plants. Plant Sci 270:292–300
Pathak RR, Ahmad A, Lochab S, Raghuram N (2008) Molecular physiology of plant nitrogen use efficiency and biotechnological options for its enhancement. Curr Sci 94:1394–1403
Pathak RR, Jangam AP, Malik A, Sharma N, Jaiswal DK, Raghuram N (2020) Transcriptomic and network analyses reveal distinct nitrate responses in light and dark in rice leaves (Oryza sativa Indica var. Panvel1). Sci Rep 10:1–17
Pathak RR, Mandal VK, Jangam AP, Sharma N, Madan B, Jaiswal DK, Raghuram N (2021) Heterotrimeric G-protein α subunit (RGA1) regulates tiller development, yield, cell wall, nitrogen response and biotic stress in rice. Sci Rep 11:1–19
Peng P, Gao Y, Li Z, Yu Y, Qin H, Guo Y, Huang R, Wang J (2019) Proteomic analysis of a rice mutant sd58 possessing a novel d1 allele of heterotrimeric G protein alpha subunit (RGA1) in salt stress with a focus on ROS scavenging. Int J Mol Sci 20:167
Prasad R, Shivay Y, Kumar D, Sharma S (2006) Learning by doing exercises in soil fertility (A practical manual for soil fertility). Division of Agronomy, IARI, New Delhi 68:
Qu C, Liu C, Gong X, Li C, Hong M, Wang L, Hong F (2012) Impairment of maize seedling photosynthesis caused by a combination of potassium deficiency and salt stress. Environ. Experim. Bot. 75:134–141
Raghuram N (2023) Reactive nitrogen in climate change, crop stress, and sustainable agriculture: a personal journey. In: Singh AK, Tuteja N (eds) Ansari MW. Global climate change and plant stress management, Wiley Online Library, pp 13–22
Raghuram N, Sharma N (2019) Improving crop nitrogen use efficiency. In: Moo-Young M (ed) Comprehensive biotechnology, 3rd edn. Elsevier, Pergamon
Raghuram N, Sopory SK (1999) Roles of nitrate, nitrite and ammonium ion in phytochrome regulation of nitrate reductase gene expression in maize. IUBMB Life 47:239–249
Raghuram N, Sutton MA, Jeffery R, Ramachandran R, Adhya TK (2021) From South Asia to the world: embracing the challenge of global sustainable nitrogen management. One Earth 4:22–27
Raghuram N, Aziz T, Kant S, Zhou J, Schmidt S (2022) Nitrogen use efficiency and sustainable nitrogen management in crop plants. Front Plant Sci 13:862091
Raudvere U, Kolberg L, Kuzmin I, Arak T, Adler P, Peterson H, Vilo J (2019) g: Profiler: a web server for functional enrichment analysis and conversions of gene lists (2019 update). Nucleic Acids Res 47:W191–W198
Sandhu N, Sethi M, Kumar A, Dang D, Singh J, Chhuneja P (2021) Biochemical and genetic approaches improving nitrogen use efficiency in cereal crops: a review. Front Plant Sci 12:657629
Sawaki N, Tsujimoto R, Shigyo M, Konishi M, Toki S, Fujiwara T, Yanagisawa S (2013) A nitrate-inducible GARP family gene encodes an auto-repressible transcriptional repressor in rice. Plant Cell Physiol 54:506–517
Shannon P, Markiel A, Ozier O, Baliga NS, Wang JT, Ramage D, Amin N, Schwikowski B, Ideker T (2003) Cytoscape: a software environment for integrated models of biomolecular interaction networks. Genome Res 13:2498–2504
Sharma N, Sinha VB, Gupta N, Rajpal S, Kuchi S, Sitaramam V, Parsad R, Raghuram N (2018) Phenotyping for nitrogen use efficiency: rice genotypes differ in N-responsive germination, oxygen consumption, seed urease activities, root growth, crop duration, and yield at low N. Front Plant Sci 9:1452
Sharma N, Sinha VB, Prem Kumar NA, Subrahmanyam D, Neeraja C, Kuchi S, Jha A, Parsad R, Sitaramam V, Raghuram N (2021) Nitrogen use efficiency phenotype and associated genes: roles of germination, flowering, root/shoot length and biomass. Front Plant Sci 11:2329
Sharma N, Kumari S, Jaiswal DK, Raghuram N (2022) Comparative transcriptomic analyses of nitrate-response in rice genotypes with contrasting nitrogen use efficiency reveals common and genotype-specific processes, molecular targets and nitrogen use efficiency-candidates. Front Plant Sci 13:881204
Shin S-Y, Jeong JS, Lim JY, Kim T, Park JH, Kim J-K, Shin C (2018) Transcriptomic analyses of rice (Oryza sativa) genes and non-coding RNAs under nitrogen starvation using multiple omics technologies. BMC Genomics 19:1–20
Stateczny D, Oppenheimer J, Bommert P (2016) G protein signaling in plants: minus times minus equals plus. Curr Opin Plant Biol 34:127–135
Shanks CM, Huang J, Cheng C-Y, Shih H-J, Brooks M, Alvarez JM, Araus V, Swift J, Henry A, Coruzzi GM (2022) Validation of a high-confidence regulatory network for gene-to-NUE phenotype in field-grown rice. Front. Plant Sci. 4710
Sun H, Qian Q, Wu K, Luo J, Wang S, Zhang C, Ma Y, Liu Q, Huang X, Yuan Q (2014) Heterotrimeric G proteins regulate nitrogen-use efficiency in rice. Nat Genet 46:652–656
Supek F, Bošnjak M, Škunca N, Šmuc T (2011) REVIGO summarizes and visualizes long lists of gene ontology terms. PLoS ONE 6:e21800
Sutton M, Raghuram N, Adhya TK, Baron J, Cox C, de Vries W, Hicks K, Howard C, Ju X, Kanter D (2019) The nitrogen fix: from nitrogen cycle pollution to nitrogen circular economy-frontiers 2018/19: emerging issues of environmental concern chapter 4. In: Frontiers 2018/19: emerging issues of environmental concern
Swain DM, Sahoo RK, Srivastava VK, Tripathy BC, Tuteja R, Tuteja N (2017) Function of heterotrimeric G-protein γ subunit RGG1 in providing salinity stress tolerance in rice by elevating detoxification of ROS. Planta 245:367–383
The SV, Snyder R, Tegeder M (2021) Targeting nitrogen metabolism and transport processes to improve plant nitrogen use efficiency. Front Plant Sci 11:628366
Thimm O, Bläsing O, Gibon Y, Nagel A, Meyer S, Krüger P, Selbig J, Müller LA, Rhee SY, Stitt M (2004) MAPMAN: a user-driven tool to display genomics data sets onto diagrams of metabolic pathways and other biological processes. Plant J 37:914–939

Tian T, Liu Y, Yan H, You Q, Yi X, Du Z, Xu W, Su Z (2017) agriGO v2.0: a GO analysis toolkit for the agricultural community, 2017 update. Nucleic Acids Res 45:W122–W129

Tian W-j, Zhang X-q, Wang X-w, Xie J, Li Y-y, Sun Y, Tao Y-r, Xiong Y-z, Sang X-c (2018) Genetic mapping and salt tolerance of a novel D1-allelic mutant of rice (Oryza sativa L.). Acta Physiol Plant 40:1–10

Tiwari R, Bisht NC (2022) The multifaceted roles of heterotrimeric G-proteins: lessons from models and crops. Planta 255(4):88

Tseng KC, Li GZ, Hung YC, Chow CN, Wu NY, Chien YY, Zheng HQ, Lee TY, Kuo PL, Chang SB (2020) EXPath 2.0: an updated database for integrating high-throughput gene expression data with biological pathways. Plant Cell Physiol 61:1818–1827

Udvardi M, Below FE, Castellano MJ, Eagle AJ, Giller KE, Ladha JK, Liu X, Maaz TM, Nova-Franco B, Raghuram N (2021) A research road map for responsible use of agricultural nitrogen. Front Sustain Food Syst 5:660155

Urano D, Colaneri A, Jones AM (2014) Gα modulates salt-induced cellular senescence and cell division in rice and maize. J Exp Bot 65(22):6553–6561

Urano D, Leong R, Wu T-Y, Jones AM (2020) Quantitative morphological phenomics of rice G protein mutants portend autoimmunity. Dev Biol 457:83–90

Vidal EA, Alvarez JM, Araus V, Riveras E, Brooks MD, Krouk G, Ruffel S, Lejay L, Crawford NM, Coruzzi GM (2020) Nitrate in 2020: thirty years from transport to signaling networks. Plant Cell 32:2094–2119

Wang D, Qin B, Li X, Tang D, Ye Zhang, Cheng Z, Xue Y (2016) Nucleolar DEAD-box RNA helicase TOGR1 regulates thermotolerant growth as a pre-rRNA chaperone in rice. PLoS Genet. 12:e1005844

Wang R, Tischner R, Gutiérrez RA, Hoffman M, Xing X, Chen M, Coruzzi G, Crawford NM (2004) Genomic analysis of the nitrate responseusing a nitrate reductase-null mutant of Arabidopsis. Plant Physiol. 136:2512–2522

Wang K, Xu F, Yuan W, Sun L, Wang S, Aslam MM, Zhang J, Xu W (2021) G protein γ subunit qPE9-1 is involved in rice adaptation under elevated CO2 concentration by regulating leaf photosynthesis. Rice 14:1–10

Warpeha KM, Lateef SS, Lapik Y, Anderson M, Lee BS, Kaufman LS (2006) G-protein-coupled receptor 1, G-protein G α-subunit 1, and prephenate dehydratase 1 are required for blue light-induced production of phenylalanine in etiolated Arabidopsis. Plant Physiol 140:844–855

Warpeha KM, Upadhyay S, Yeh J, Adamiak J, Hawkins SI, Lapik YR, Anderson MB, Kaufman LS (2007) The GCR1, GPA1, PRN1, NF-Y signal chain mediates both blue light and abscisic acid responses in Arabidopsis. Plant Physiol 143:1590–1600

Xing J, Cao X, Zhang M, Wei X, Zhang J, Wan X (2022) Plant nitrogen availability and crosstalk with phytohormones signalings and their biotechnology breeding application in crops. Plant Biotechnol. J. 21:1320–1342

Xu G, Takahashi H (2020) Improving nitrogen use efficiency: From cells to plant systems. Oxford University Press, pp 4359–4364

Yadav DK, Shukla D, Tuteja N (2013) Rice heterotrimeric G-protein alpha subunit (RGA1): in silico analysis of the gene and promoter and its upregulation under abiotic stress. Plant Physiol Biochem 63:262–271

Yantong L, Ting L, Zhishu J, Chuihai Z, Rong H, Jiao Q, Xiaoli L, Limei P, Yongping S, Dahu Z, Yicong C, Changlan Z, Junru F, Haohua H, Jie X (2022) Characterization of a novel weak allele of *RGA1*/*D1* and its potential application in rice breeding. Rice Sci 29(6):522–534

Yang X, Xia X, Zhang Z, Nong B, Zeng Y, Xiong F, Wu Y, Gao J, Deng G, Li D (2017) QTL mapping by whole genome re-sequencing and analysis of candidate genes for nitrogen use efficiency in rice. Front. Plant Sci. 8:1634

Yang SY, Hao DL, Song ZZ, Yang GZ, Wang L, Su YH (2015) RNA-Seq analysis of differentially expressed genes in rice under varied nitrogen supplies. Gene 555:305–317

Zait Y, Ferrero-Serrano Á, Assmann SM (2021) The α subunit of the heterotrimeric G protein regulates mesophyll CO2 conductance and drought tolerance in rice. New Phytol 232:2324–2338

Zhang L, Hu G, Cheng Y, Huang J (2008) Heterotrimeric G protein α and β subunits antagonistically modulate stomatal density in *Arabidopsis thaliana*. Dev Biol 324:68–75

Zhang H, Xie P, Xu X, Xie Q, Yu F (2021) Heterotrimeric G protein signalling in plant biotic and abiotic stress response. Plant Biol 23:20–30

Zhao Z, Stanley BA, Zhang W, Assmann SM (2010) ABA-regulated G protein signaling in Arabidopsis guard cells: a proteomic perspective. J Proteome Res 9:1637–1647

Zhu Y, Li T, Xu J, Wang J, Wang L, Zou W, Zeng D, Zhu L, Chen G, Hu J (2020) Leaf width gene LW5/D1 affects plant architecture and yield in rice by regulating nitrogen utilization efficiency. Plant Physiol Biochem 157:359–369